D17 target cells ($2 \times 10^5$ cells/60 mm dish) in the presence of polybrene. The infected D17 cells were selected for resistance to G418 (400 μg/ml) in the presence of 1 μM AZT to suppress reinfection, and characterized by staining with 5-bromo-4-chloro-3-indoyl-β-D-galacto-pyranoside (X-Gal) ~2 weeks after G418 selection. The frequencies of inactivating mutations in *lacZ* quantified as described before (blue versus white colonies) (34).

### Processivity of DNA synthesis—trap assay

Processivity reactions were carried out in Reaction Buffer containing 20 nM $T_{d100}/P_{d18}$, 100 μM of each dNTP, 30 nM HIV-1 RT, 50 nM MoMLV RT or 100 nM XMRV RT and 1 μg/μl unlabeled calf thymus DNA trap in 50 μL. Enzymes were pre-incubated with $T_{d100}/P_{d18}$ for 1 min before adding dNTPs (100 μM each) together with the calf thymus DNA trap. Reactions were incubated at 37°C, and 10 μl aliquots were taken out at 3, 7.5 and 15 min for HIV-1 RT or at 7.5, 15 and 30 min for XMRV RT and MoMLV RT, and mixed with equal volume of loading dye. The effectiveness of the trap was determined by pre-incubating the enzyme with the trap before adding $T_{d100}/P_{d18}$. Control DNA synthesis was measured in absence of trap under the same conditions. Reaction products were resolved as above.

### Single turnover processivity assays

Thirty nanomolar $T_{d31}/5'$-Cy3-$P_{d18a}$ was pre-incubated for 10 min with 100 nM XMRV or 50 nM MoMLV RT in Reaction Buffer, then rapidly mixed with 100 μM dNTPs, 5 mM $MgCl_2$ for varying times (0.1–45 s) before quenching with EDTA (50 mM final). Single turnover processivity of HIV-1 RT was assayed with 40 nM enzyme, 20 nM DNA and 50 μM of each nucleotide were used. The reaction products were resolved and quantified as described above. The data were fit to a one-phase exponential decay equation for the elongation of the 18-mer primer. The rates of appearance and extension of products from subsequent nucleotide incorporations (19- and 27-mer) were obtained by fitting the intensities of corresponding bands to double exponential (Equation 4):

$$P = A(1 - e^{-k_1 t}) + (e^{-k_2 t}) + C \quad (4)$$

where A is the amplitude, P is the amount of 19-mer, 20-mer or higher length products, $k_1$ is the rate of product generation, $k_2$ the rate of subsequent elongation and C a constant (29,35).

### Assays for reverse transcriptase inhibition

DNA synthesis by 50 nM XMRV RT or MoMLV RT was carried out in Reaction Buffer using 20 nM $T_{d100}/5'$-Cy3-$P_{d18a}$, 2.5 μM dNTP, 5 mM $MgCl_2$ and varying amounts of NRTI (0–100 μM). Reactions were quenched with 95% formamide after 1 h incubation at 37°C (38). In experiments with aptamers 10 nM XMRV RT, 20 nM $T_{d31}/5'$-Cy3-$P_{d18a}$ and 50 μM dNTPs were used in the presence of varying amounts of aptamer for 30 min (0–500 nM for m.1.3; 0–25 nM for m.1.4 and m.1.1FL). The inhibition of DNA polymerization was monitored by resolving the products on 15% polyacrylamide–7 M urea gels and visualized as described above. Bands corresponding to full extension products were quantified using MultiGauge Software and $IC_{50}$s were obtained from dose–response curves using GraphPad Prism.

### PPi- and ATP-dependent excision and rescue of $T/P_{AZT\text{-}MP}$ or $T/P_{EFdA\text{-}MP}$

The ability of enzymes to use PPi or ATP to unblock template-primers that had AZT-MP ($T/P_{AZT\text{-}MP}$) or EFdA-MP ($T/P_{EFdA\text{-}MP}$) at their 3′ primer ends was measured as follows: 20 nM of $T/P_{AZT\text{-}MP}$ or $T/P_{EFdA\text{-}MP}$ were prepared as described before (32). They were incubated at 37°C with either 60 nM HIV-1 RT or 200 nM XMRV RT in the presence of 0.15 mM PPi or 3.5 mM ATP for PPi- or ATP-dependent rescue reactions, respectively. Reactions were initiated by the addition of $MgCl_2$ (6 mM). Aliquots were removed at different times (0–90 min) and analyzed as above. Rescue assays were performed in the presence of 100 μM dATP to prevent EFdA-MP reincorporation, 0.5 μM dTTP, 10 μM ddGTP and 10 mM $MgCl_2$.

### Molecular modeling

The sequence of XMRV RT from the VP62 clone was aligned with that of MoMLV RT (PDB: 1RW3) (21,22) using ClustalW. To generate the homology model of XMRV RT, we used the Prime protocol of the Schrödinger software suite (Schrödinger Inc. NY). The resulting molecular model was further energy minimized by OPLS2005 force field using the Impact option of Schrödinger. The final model was validated with PROCHECK v.3.5.4.

## RESULTS

### Comparison of RT sequences

The XMRV and MoMLV enzymes are closely related (~95% sequence identity) with most of the differences between them being in the RNase H domain (Supplementary Figure S1). While XMRV and MoMLV differ significantly from HIV-1 RT, the known polymerase motifs (A–F) are well conserved in all three enzymes (Supplementary Figure S1). Specifically, the active site aspartates in Motifs A and C (Figure 9) (D150, D224, D225 in XMRV RT; D150, D224, D225 in MoMLV RT; D110, D185, D186 in HIV-1 RT) are conserved in all three RTs. Also, the three enzymes are similar in Motif B, which is involved in dNTP binding and multidrug resistance (AZT and dideoxy-nucleoside drugs) through the decreased incorporation mechanism (27,39–41). Specifically, all three enzymes have a glutamine at the start of this motif (Q151 in HIV-1 RT, Q190 in XMRV RT and Q190 in MoMLV RT). Motif D includes HIV-1 RT residues L210 and T215, which when mutated they enhance excision of AZT from the AZT-terminated primer terminus. This motif is mostly different in XMRV and MoMLV RTs, where the corresponding residues are N226 and A231 (Supplementary Figure S1). K219 of HIV-1 RT Motif D is proximal to

the dNTP-binding pocket and is also conserved in the other enzymes (K235). The DNA primer grip (Motif E) (36,42) in HIV-1 RT ($M_{230}G_{231}Y_{232}$) is slightly different in the gammaretroviral enzymes ($L_{245}G_{246}Y_{247}$). Motif F at the fingers subdomain of all enzymes has two conserved lysines that bind the triphosphate of the dNTP (K65 and K72 in HIV-1 RT; K103 and K110 in XMRV and MoMLV RTs).

Several HIV-1 residues involved in NRTI resistance have the resistance mutations in XMRV and MoMLV RTs (Table 1). Hence, XMRV and MoMLV RTs have a Val as the X residue (codon 223) of the conserved YXDD sequence of Motif C. An M184V mutation at this position in HIV-1 RT causes strong, steric hindrance-based, resistance to 3TC and FTC (43–45), and to a lesser extent to ddI, ABC [reviewed in (46)], and translocation defective RT inhibitors (TDRTIs) (43) (Table 1). Similarly, the M41L mutation, which causes excision-based AZT resistance in HIV is already present in XMRV and MoMLV RT (L81, Table 1). The gammaretroviral enzymes differ from HIV-1 RT in several other HIV drug resistance sites (HIV residues 62, 67, 69, 70, 75, 77, 115, 210, 215) (Table 1). Finally, there are also differences in residues that are essential for NNRTI binding in HIV-1 RT: W229 changes to Y268 in XMRV RT, Y181 to L220, Y188 to L227 and G190 to A229 (Table 1) (27,28,47–49).

## Preparation of MoMLV and XMRV RTs

The sequence coding for full-length XMRV RT from the VP-62 clone (NCBI RefSeq: NC_007815) (1) was optimized for expression in bacteria, synthesized by Epoch Biolabs and cloned as described in 'Materials and Methods' section. Both XMRV RT and MoMLV RT were tagged with a hexahistidine sequence at the N-terminus and expressed with a yield of ~2 mg/l of culture. Purified enzymes (>95% pure, Supplementary Figure S2) were stored at −20°C. The presence of NP-40 or glycerol was critical for enzyme stability.

## Steady state kinetics of nucleotide incorporation

Initial polymerase activity assays using $T_{d31}$/5′-Cy3-$P_{d18a}$ displayed overall slower polymerase activity of XMRV RT compared to HIV-1 and MoMLV RTs. This observation led us to investigate the steady state nucleotide incorporation properties of XMRV RT using single nucleotide incorporation assays. The estimated values for $k_{cat}$ (19.9 $min^{-1}$ for HIV-1 RT (32), 3.3 $min^{-1}$ for MoMLV RT, 0.6 $min^{-1}$ for XMRV RT) and $K_{m.dNTP}$ (0.07 μM for HIV-1 RT (32), 3.3 μM for MoMLV RT, 3.0 μM for XMRV RT) show that XMRV RT has a drastically reduced efficacy ($k_{cat}/K_{m.dNTP}$) at nucleotide incorporation, compared to both MoMLV and HIV-1 RTs.

## DNA binding affinity

To assess if the efficiency of XMRV RT was also affected by a lower DNA binding affinity we measured the DNA binding affinity of the enzymes using three methods: gel-mobility shift assays, pre-steady state kinetics and SPR. Gel-mobility shift assays showed that the $K_{D.DNA}$ for XMRV RT was marginally higher than that for HIV-1 RT and MoMLV RT (data not shown) (50) suggesting weaker binding to DNA.

## DNA binding affinity using pre-steady state kinetics

Pre-steady state kinetics allows estimation of the fraction of active polymerase sites as well as the $K_{D.DNA}$ value for the enzyme. The amplitudes of DNA extensions using XMRV RT and/or MoMLV RT at varying DNA concentrations were plotted against the DNA concentration and

**Table 1.** HIV-1 RT drug resistance mutations with wild-type XMRV RT and MoMLV RT residues

| | HIV-1 residue numbers | HIV-1 RT wt | HIV-1 resistance mutations | | | | | XMRV RT wt | MoMLV RT wt |
|---|---|---|---|---|---|---|---|---|---|
| | | | 3TC | ABC | TDF | D4T | EFdA | | |
| Thymidine analog mutations (TAMs) | 184 | M | V | V | – | – | V | V223 | V223 |
| | 41 | M | – | L | L | L | – | L81 | L81 |
| | 67 | D | – | N | N | N | – | G105 | G105 |
| | 210 | L | – | W | W | W | – | N226 | N226 |
| | 215 | T | – | FY | FY | FY | – | A231 | A231 |
| | 219 | K | – | | | QE | – | K235 | K235 |
| Non-thymidine analog regimen mutations | 65 | K | RN | RN | RN | RN | – | K103 | K103 |
| | 70 | K | EG | EG | EG | – | – | D108 | D108 |
| | 74 | L | – | VI | – | – | – | V112 | V112 |
| | 75 | V | – | TM | M | TM | – | Q113 | Q113 |
| | 115 | Y | – | F | F | | – | F155 | F155 |
| | 69 | T | Ins | Ins | Ins | Ins | – | N107 | N107 |
| Multi-NRTI resistance mutations | 151 | Q | M | M | M | M | – | Q190 | Q190 |
| | 62 | A | V | V | V | V | – | P104 | P104 |
| | 75 | V | – | I | – | I | – | Q113 | Q113 |
| | 77 | F | – | L | – | L | – | L115 | L115 |
| | 116 | F | – | Y | – | Y | – | F156 | F156 |
| TDRTI Mutations | 184 | M | V | V | – | – | V | V223 | V223 |
| | 165 | T | – | – | – | – | R | H204 | H204 |

The HIV-1 RT data are based on data from the Stanford HIV Database (85).
wt = wild-type.

the data were fit to the quadratic equation (Equation 2), yielding a $K_{D.DNA}$ of 33 nM for XMRV RT, 19 nM for MoMLV RT (Table 2) and 12.5 nM for HIV-1 RT (32). These values did not change significantly when tested with DNA of different lengths (data not shown). Hence, the transient kinetic experiments confirmed the findings of the gel-mobility shift assays showing XMRV RT to have lower DNA binding affinity than HIV-1 RT.

### Binding kinetics of XMRV and HIV-1 RT to double-stranded DNA

Measurements of $K_{D.DNA}$ using gel-mobility shift assays and pre-steady state kinetic methods do not offer insights regarding the kinetics of binding and release of nucleic acid from the viral polymerases. Hence, we used SPR to measure directly DNA binding and the DNA dissociation components of the $K_{D.DNA}$. We attached on the SPR chip a nucleic acid biotinylated at the 5′ template end and immobilized it on a streptavidin sensor chip. Various concentrations of either XMRV or HIV-1 RT were flowed over the chip to measure the association ($k_{on}$) and dissociation ($k_{off}$) rates of the enzymes in real time (Figure 1). HIV-1 RT had considerably slower dissociation rates than XMRV RT, and longer dissociation phases were needed to obtain reliable values.

Several methods were tested to best fit our data. The 'heterogeneous ligand' method gave the best fit for both XMRV and HIV-1 RT. In this model the $x^2$ values for DNA binding to XMRV and HIV-1 RT were 9.3 $RU^2$ and 48.1 $RU^2$, respectively, compared to 15.1 $RU^2$ and 152 $RU^2$ when we tried fitting the data in a 'homogeneous ligand' model. The former model assumes that RT binds DNA in two different modes and provides two association ($k_{on}$) and two dissociation constants ($k_{off}$).

Our data show that XMRV RT has a slightly faster rate of association ($k_{on}$) than HIV-1 RT. We measured two $k_{on}$ values of $7.3 \times 10^6 M^{-1}s^{-1}$ and $8.2 \times 10^4 M^{-1}s^{-1}$ for XMRV RT versus $7.6 \times 10^5 M^{-1}s^{-1}$ and $1.2 \times 10^6 M^{-1}s^{-1}$ for HIV-1 RT. Interestingly, the dissociation rate of XMRV RT was significantly faster than that of HIV-1 RT ($0.28\,s^{-1}$ and $0.0045\,s^{-1}$ for XMRV RT and $7.8 \times 10^{-4}$ $s^{-1}$and $0.0076\,s^{-1}$ for HIV-1 RT) (Table 3). This difference in dissociation rate resulted in a $K_{D.DNA}$ at least 1 order of magnitude higher for XMRV RT compared to HIV-1 RT (38 and 54 nM versus 1.0 and 6.1 nM for XMRV and HIV-1 RT, respectively) (Table 3).

**Table 2.** Kinetic parameters of DNA binding and synthesis by HIV-1 and XMRV RTs

| Nucleotide affinity and incorporation | HIV-1 RT[a] | MoMLV RT | XMRV RT |
|---|---|---|---|
| $K_{d.dNTP}$ (μM) | 1.3 ± 0.4 | 25 ± 5.3 | 26.6 ± 6.5 |
| $k_{pol}$ ($s^{-1}$) | 24.4 ± 0.9 | 14.1 ± 0.8 | 8.9 ± 0.6 |
| $k_{pol}/K_{d.dNTP}$ ($s^{-1}\cdot\mu M^{-1}$) | 18.8 | 0.56 | 0.33 |
| DNA binding affinity: | | | |
| $K_{D.DNA}$ (nM) | 12.5 | 19.0 | 32.5 |

[a]HIV-1 RT data published previously (29).

### Nucleotide binding affinity and optimal incorporation efficiency

A transient-state kinetics approach was used to estimate the dNTP binding affinity ($K_{d.dNTP}$) and maximum nucleotide incorporation rate ($k_{pol}$) (55). The rates at varying concentrations of next incoming nucleotide (dATP) were determined by plotting the amount of extended primer as a function of time. The rates were then plotted against dATP concentration. The data were fit to a hyperbola (Equation 3). The $K_{d.dNTP}$ for XMRV RT is 26.6 μM and the $k_{pol}$ is $8.9\,s^{-1}$ (Figure 2) (Table 2). Under similar conditions the $K_{d.dNTP}$ and $k_{pol}$ were 1.3 μM and $24.4\,s^{-1}$ for HIV-1 RT (29) and 25 μM and $14.1\,s^{-1}$ for MoMLV RT.

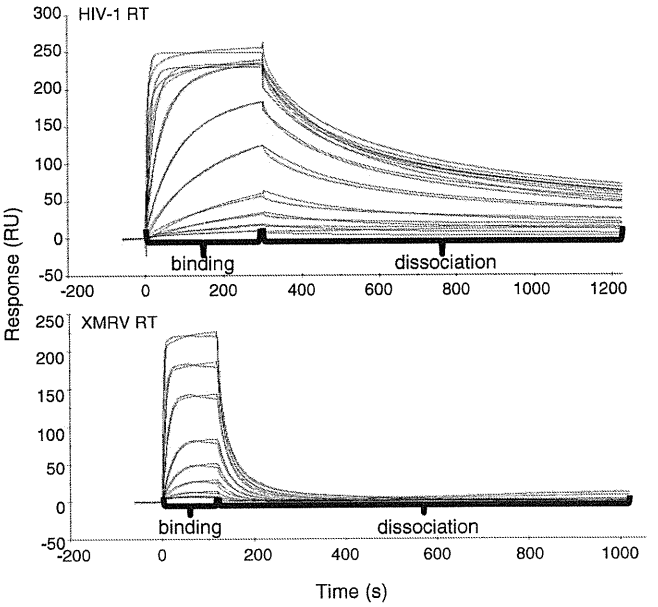


**Figure 1.** Assessment of $K_{D.DNA}$, $k_{on}$ and $k_{off}$ using surface plasmon resonance. SPR was used to measure the binding affinity of RTs to a nucleic acid substrate. Increasing concentrations of each RT (0.2, 0.5, 1, 2, 5, 10, 20, 50, 100 and 200 nM) were injected over a streptavidin chip with biotinylated double-stranded DNA immobilized on its surface as described in 'Materials and Methods' section. The experimental trace (red) shown is the result of a subtraction of the data obtained from the channel containing the immobilized nucleic acid minus the signal obtained from an empty channel. The black curve represents the fitted data according to the 'heterogeneous ligand' model that assumes two different binding modes for RT on the nucleic acid.

**Table 3.** DNA binding constants for HIV-1 and XMRV RTs from surface plasmon resonance

| | HIV-1 RT | XMRV RT |
|---|---|---|
| $k_{on}$ ($M^{-1}.s^{-1}$) | $7.6 \times 10^5$ | $7.3 \times 10^6$ |
| $k_{off}$ ($s^{-1}$) | $7.8 \times 10^{-4}$ | $2.8 \times 10^{-1}$ |
| $K_{D.DNA1}$ (nM) | 1 | 38 (38-fold)[a] |
| $k_{on}$ ($M^{-1}.s^{-1}$) | $1.2 \times 10^6$ | $8.2 \times 10^4$ |
| $k_{off}$ ($s^{-1}$) | $7.6 \times 10^{-3}$ | $4.5 \times 10^{-3}$ |
| $K_{D.DNA2}$ (nM) | 6.1 | 54 (9-fold)[a] |

[a]Increase in $K_{D.DNA}$ (decrease in affinity) with respect to HIV-1 RT. ($K_{D1\text{-}XMRV\ RT}/K_{D1HIV\text{-}1\text{-}RT}$ and $K_{D2\text{-}XMRV\ RT}/K_{D2HIV\text{-}1\text{-}RT}$).

### Fidelity of nucleotide incorporation

To assess whether XMRV RT displays high nucleotide incorporation fidelity we monitored the incorporation of three dNTPs by XMRV RT and compared with HIV-1 RT (52). The results of fidelity assay are shown in Figure 3. The lanes marked '4dNTPs' for all enzymes represent the DNA synthesis using a $T_{d100}/5'$-Cy3-$P_{d18a}$ template-primer in the presence of all four dNTPs. The subsequent lanes, marked '-dNTP', correspond to the synthesis of DNA in the absence of that specific deoxynucleotide triphosphate. The comparison of the DNA synthesis in the absence of one nucleotide by HIV-1 RT, MoMLV RT and XMRV RT shows that HIV-1 and MoMLV RTs were able to misincorporate and extend the primer beyond the missing nucleotide more efficiently than XMRV RT, suggesting that the latter is a less error prone DNA polymerase. It should be noted that the higher fidelity of XMRV is not the result of measuring a smaller number of errors because of the decreased replication rate, as the assay conditions were optimized to allow production of the same amount of full length product in the presence of all four dNTPs for and MoMLV RTs. To further investigate the fidelity of DNA synthesis by XMRV RT, the kinetics of mismatch nucleotide incorporation were carried out in a quantitative manner by monitoring the incorporation of single mismatched nucleotide under pre-steady state conditions. The estimated $K_{D.dTTP}$ (mismatch) and $k_{pol}$ values show that XMRV RT has a lower affinity for a mismatched nucleotide but comparable turnover number than MoMLV RT, suggesting that the observed higher fidelity over MoMLV RT is due to differences during the nucleotide-binding step (Table 4). However, compared to HIV-1 RT, XMRV RT has decreased both affinity and incorporation rate, suggesting that its higher fidelity is the result of both decreased binding of mismatched nucleotides and slow rate of incorporation.

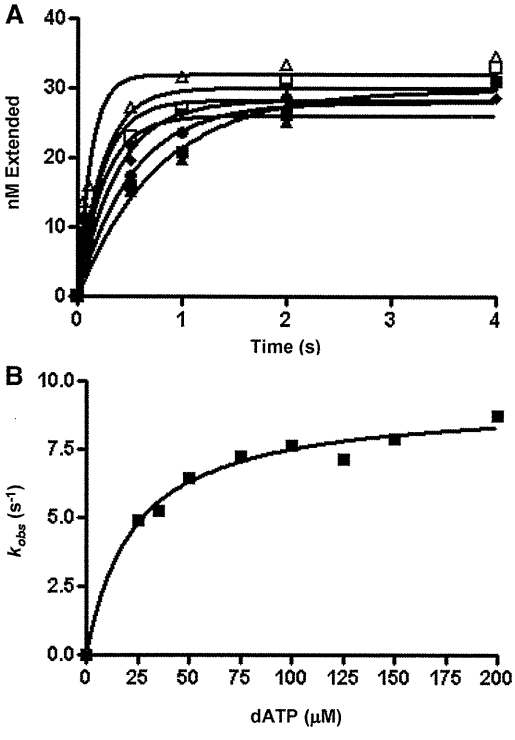


**Figure 2.** Pre-steady state kinetics of nucleotide incorporation by XMRV RT. 150 nM XMRV RT was pre-incubated with 40 nM $T_{d31}/5'$-Cy3-$P_{d18a}$ rapidly mixed with a solution containing $MgCl_2$ (5 mM) and varying concentrations of dATP: 25 μM (filled square), 35 μM (filled triangle), 50 μM (filled inverted triangle), 75 μM (filled rhombus), 100 μM (filled circle), 125 μM (open square) and 150 μM (open triangle); and incubated for 0.1 to 6 s before being quenched with EDTA. The DNA product for each dATP concentration was fit to the burst equation (**A**). The burst amplitudes generated for each dATP concentration were then fit to a hyperbola equation (**B**) yielding the optimal rates of dNTP incorporation; $k_{pol}$ ($8.9\ s^{-1}$) and dNTP binding to the RT-DNA complex; $K_{d.dATP}$ (26.6 μM).

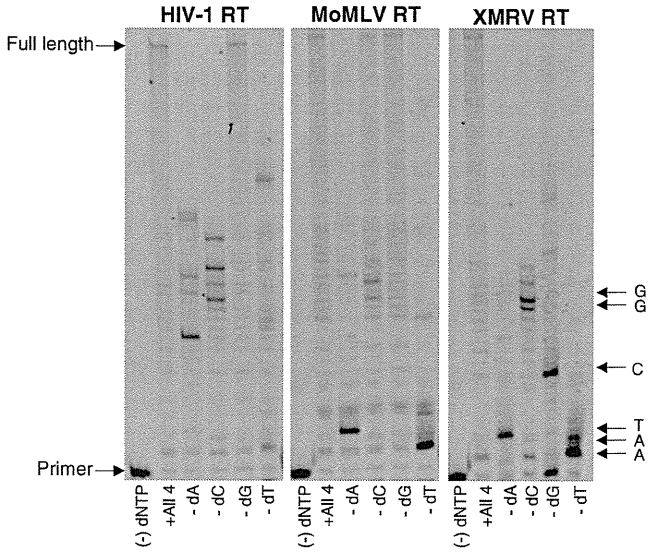


**Figure 3.** Comparison of *in vitro* fidelity of HIV-1, MoMLV and XMRV RTs. Extension of 10 nM $T_{d100}/5'$-Cy3-$P_{d18a}$ by HIV-1 RT, MoMLV RT or XMRV RT (20, 50 and 50 nM, respectively) in the presence of 150 μM each of three out of four nucleotides (the missing nucleotide is marked at the bottom of each lane). Reactions were run for 30 min for HIV-1 RT and 45 min for XMRV RT and MoMLV RT. For each enzyme the first lane in each set shows the position of unextended primer, the second lane shows full extension in the presence of all four dNTPs, and each consecutive lane shows extension in the presence of three dNTPs. The arrows on the right mark the expected pauses based on the indicated composition of the template strand.

**Table 4.** Kinetics of mismatch incorporation for HIV-1, MoMLV and XMRV RTs

| Enzyme | HIV-1 RT | MoMLV RT | XMRV RT |
|---|---|---|---|
| $K_{d.dNTP}$ (μM) | 9 ± 0.3 | 38.9 ± 11.6 | 256 ± 72 |
| $k_{pol}$ ($s^{-1}$) | 6.81 ± 1.2 | 0.16 ± 0.01 | 0.15 ± 0.018 |
| $k_{pol}/K_{d.dNTP}$ ($s^{-1} \cdot \mu M$) | 0.756 | 0.0041 | 0.00058 |
| Fidelity[a] | 0.04 | 0.007 | 0.002 |

[a]Fidelity is the ratio of the incorporation efficiency ($k_{pol}/K_{d.dNTP}$) of the mismatched nucleotide (dTTP) over that of the correct (dATP) ([$k_{pol}/K_d$]dTTP/[$k_{pol}/K_d$]dATP).

### Intracellular fidelity by measuring LacZ mutation frequency

The ANGIE P cells used for this assay are a D17-based encapsidating cell line and contain an MLV-based retroviral vector (GA-1), which encodes a bacterial β-galactosidase gene (*lacZ*) and a neomycin phosphotransferase gene (*neo*). Replication fidelity is a measure of the frequency of *lacZ* inactivation and was determined by measuring *lacZ* non-expressing white colonies. The results show that the number of white colonies was not statistically different in the case of XMRV as compared to AM-MLV, suggesting that under these conditions the fidelity of XMRV is not significantly different than that of AM-MLV (Figure 4).

### Processivity of DNA synthesis

Processivity is the probability of translocation of a polymerase along a template and predicts the number of cycles of nucleotide incorporation during one productive enzyme–DNA binding event. We assessed XMRV RT's processivity of DNA synthesis in comparison to HIV and MoMLV RTs using both a gel-based trap assay and a quantitative pre-steady state assay. In the gel-based assay, the enzymes were pre-incubated with template-primer, then the reaction was initiated by the addition of all four nucleotides together with calf thymus DNA, which was used as a trap to bind free enzyme dissociated from the substrate during the course of the reaction (38). The length of the DNA product is an inverse measure of termination probability, as previously described. As a control, we used lanes where no trap was present; establishing that the same amount of total polymerase activity (processive and non-processive) is provided in all cases. The results indicate that XMRV RT is less processive than HIV-1 and MoMLV RTs with shorter DNA product after 30 min of reaction in the presence of trap (Figure 5).

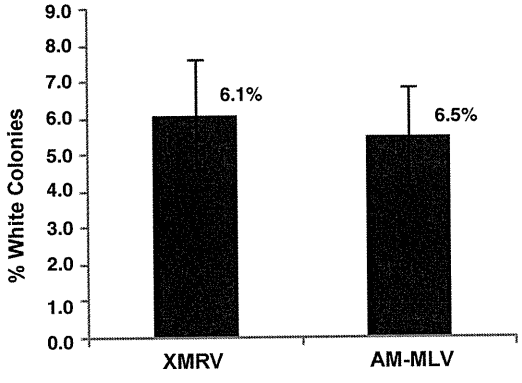


**Figure 4.** Comparison of *in vivo* fidelity of XMRV with amphotropic MLV. The ANGIE P cells used for this assay contain a retroviral vector (GA-1), which encodes a bacterial β-galactosidase gene (*lacZ*) and a neomycin phosphotransferase gene. Replication fidelity is measured by the frequency of *lacZ* inactivation resulting in an increase in white colonies. The fidelity differences between the two viruses are not statistically significant (error bars represent standard error from three independent experiments).

To measure processivity quantitatively we applied a single turnover processivity assay developed by Patel *et al.* (35) (Figure 6). In this assay, the rates of consecutive nucleotide incorporations under single turnover conditions are monitored. The rate of elongation incorporation ($k_1$) and the rate of processive DNA synthesis ($k_2$) (Equation 4) were calculated at several template positions for each enzyme. The ratio of the rate of processive DNA synthesis to the rate of nucleotide incorporation ($k_2/k_1$) is referred to as the processivity index (35). The absolute values of these constants for HIV-1 RT, XMRV and MoMLV RT and their ratios are collected in Table 5. XMRV RT is clearly the least processive for each extension product. The difference in processivity varies significantly depending on sequence or sequence context (decrease in processivity from 3-fold up to 10-fold). While the current data do not allow generalization of rules for pausing at specific sites, this clearly shows consistently that XMRV is not as efficient as MoMLV RT in polymerizing processively through 'difficult spots'.

### Susceptibility of XMRV RT to NRTIs, TDRTIs and NNRTIs

Previous studies have shown that XMRV is inhibited by some antivirals (53–56). However, the susceptibility of XMRV RT has not been tested against a wide variety of

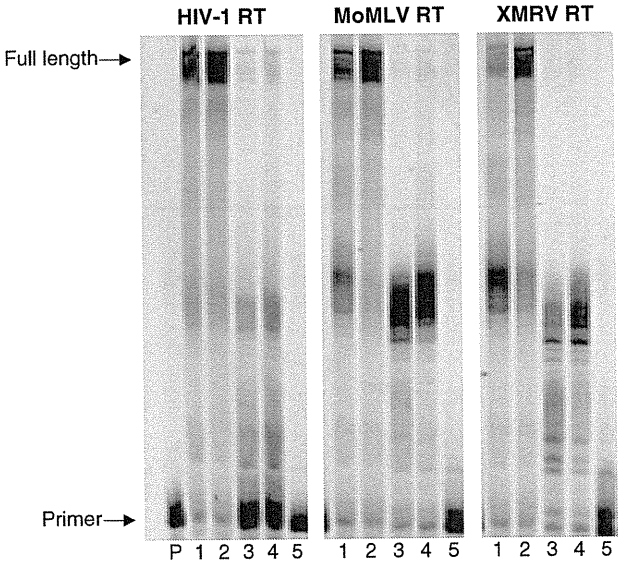


**Figure 5.** Processivity (trap assay) of HIV-RT, MoMLV RT and XMRV RT. DNA synthesis was monitored in the presence of calf thymus DNA as an enzyme trap. Each enzyme (30 nM HIV RT, 100 nM MoMLV RT or 100 nM XMRV RT) was pre-incubated with 40 nM $T_{d100}$/Cy3-$P_{d18a}$. Lanes 1 and 2 of each set show unlimited DNA synthesis in the absence of trap for 5 and 10 min for HIV-1 RT and 10 and 40 min for XMRV RT and MoMLV RT. In Lanes 3 and 4 the reaction is initiated by the addition of dNTPs (100 μM each) together with the calf thymus DNA trap (0.5 μg/μl) such that the products generated represent a single processive synthesis event for the respective time points for each enzyme. Lane 5 shows the effectiveness of the trap determined by incubating the calf thymus DNA with the enzyme before addition of labeled template-primer. Processive primer extension by HIV-1 RT and MoMLV RT in Lanes 4–6 of the left and middle panel is higher than by XMRV RT in Lanes 4–6 of the right panel.

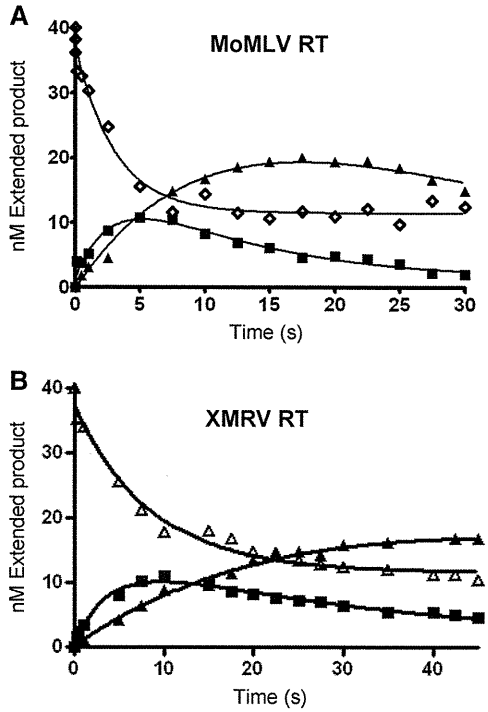


**Figure 6.** Single-turnover processivity assays. 30 nM $T_{d31}$/Cy3-$P_{d18a}$ was combined with 100 nM XMRV RT or 50 nM MoMLV RT in RT buffer before rapidly mixing with all four dNTPs (100 μM each) and 5 mM $MgCl_2$ for varying incubation times (0.05–45 s) and quenching with EDTA. Extension of the 18-mer primer (open rhombus) ((open triangle) for XMRV RT) into 19-mer (filled square) and 22-mer (filled square), by MoMLV RT (**A**) and XMRV RT (**B**) was fit to a double exponential equation to determine rates of product appearance, and subsequent processive extension of those products (rates shown in Table 5).

**Table 5.** Single turnover processivity parameters of HIV-1, MoMLV and XMRV RTs

| Template site | Processivity index ($k_2/k_1$) | | |
|---|---|---|---|
| | HIV-1 RT | MoMLV RT | XMRV RT |
| 1 | 6.98 | 0.31 | 0.12 |

1
3′-CAT TGA CAA GCT CGT GGT TAC GAT CGA TAC C
5′-Cy3-GTA ACT GTT CGA GCA CCT
The template site position monitored is underlined and labeled.

nucleoside RT inhibitors (NRTIs) that block replication by chain-terminating the primer, or by preventing translocation after their incorporation into the nascent DNA chain (TDRTIs) (32,57,58). In addition, the susceptibility of XMRV RT to non-nucleoside RT inhibitors (NNRTIs) or RNA aptamers that can be selected to block reverse transcriptases (59–63) has not been established.

Hence, we performed gel-based primer extension assays in the presence of various inhibitors. As shown in Table 6, most of the HIV-1 RT inhibitors also block XMRV RT with significantly varying $IC_{50}$s. The most potent inhibitors tested were ENdA (4′-ethynyl-2-amino-2′-deoxyadenosine) followed by EFdA. EFdA was also potent at

**Table 6.** Inhibition of XMRV and MoMLV RTs

| Compound | $IC_{50}$ (μM) | |
|---|---|---|
| | XMRV RT | MoMLV RT |
| Adefovir-DP | 0.92 | 1.02 |
| Tenofovir-DP | 6.4 | 1.51 |
| D4T-TP | 0.77 | 2.37 |
| 3TC-TP | 21 | 10 |
| EFdA-TP | 0.43 | 0.29 |
| ENdA-TP | 0.14 | 0.18 |

D4T, stavudine or 2′,3′-dehydro-2′,3′-deoxythymidine; 3TC, lamivudine; EFdA, 4′-ethynyl-2-fluoro-2′-deoxyadenosine; ENdA, 4′-ethynyl-2-amino-2′-deoxyadenosine.

inhibiting wild-type XMRV replication in cell culture with an $EC_{50}$ of 40 nM from three independent experiments (standard error was 10 nM).

Unlike HIV-1 RT, XMRV RT and MoMLV RT lack the two tyrosine residues (Y181 andY188 in HIV-1 RT) (Supplementary Figure S1) that are known to contribute to NNRTI binding. Hence, the gammaretroviral enzymes were not inhibited by the NNRTIs tested (TMC-125 and efavirenz) (Supplementary Figure S3).

## Susceptibility of XMRV RT to RNA aptamers

We also tested XMRV RT's susceptibility to three independent RNA aptamers that had been previously selected against MoMLV RT (60). The aptamers inhibited XMRV RT to varying extents with $IC_{50}$s ranging from 2 to 52 nM (Figure 7). Most notable was the m.1.1FL aptamer which gave $IC_{50}$s of 2 and 4 nM for XMRV RT (Figure 7) and MoMLV RT respectively, without inhibiting HIV-1 RT (data not shown). These inhibition assays utilized truncated forms of aptamers m.1.3 and m.1.4 lacking the original primer-binding segments of the aptamers, demonstrating that these 5′ and 3′ segments are not required.

## PPi-mediated excision activity of XMRV RT

A key mechanism of NRTI resistance in HIV-1 RT is based on inhibitor excision from the primer end, using a pyrophospholytic reaction (64,65). The pyrophosphate donor *in vivo* is likely to be ATP, although PPi can efficiently unblock NRTI-terminated primers. This excision activity is present in wild-type HIV-1 RT, and is enhanced in the presence of AZT-resistance mutations. We measured the ability of wild-type XMRV to unblock primers terminated with AZT or EFdA in the presence of PPi. We found that unlike HIV-1 RT that excised AZT-MP efficiently under these conditions, XMRV RT had considerably lower excision activity (Figure 8). Similar excision experiments where ATP was used instead of PPi showed that XMRV is very inefficient in ATP-based excision as compared to HIV-1 RT (data not shown).

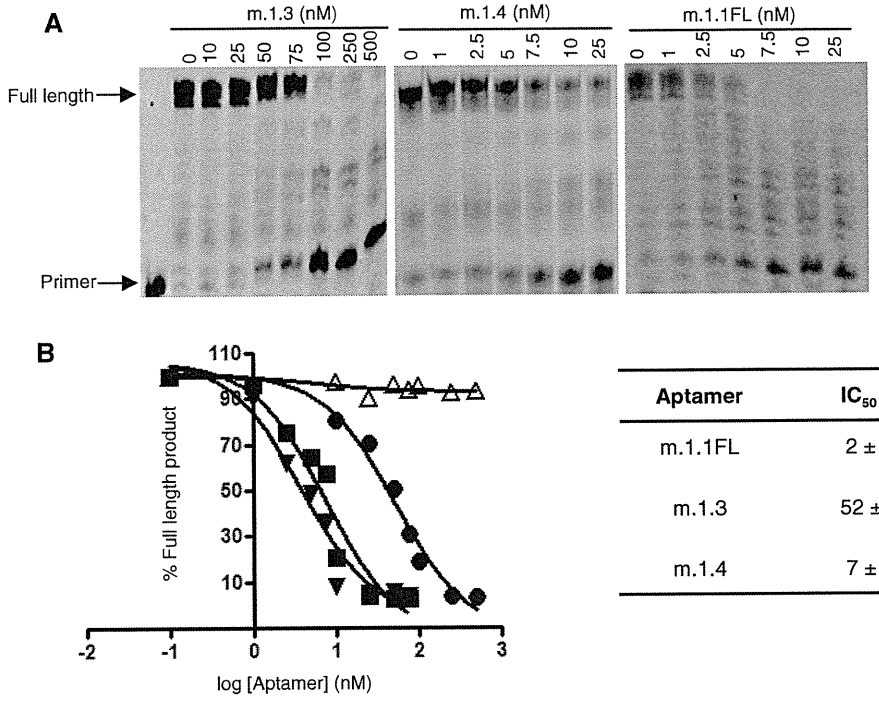


| Aptamer | $IC_{50}$ (nM) |
|---|---|
| m.1.1FL | 2 ± 0.15 |
| m.1.3 | 52 ± 0.27 |
| m.1.4 | 7 ± 0.16 |

**Figure 7.** Inhibition of XMRV RT by RNA aptamers. 10 nM XMRV RT was incubated with increasing amounts of RNA aptamer in Reaction Buffer for 5 min at 37°C followed by addition of 20 nM $T_{d31}$/Cy3-$P_{d18a}$ and 50 μM of each dNTP. (**A**) The reactions were stopped after 30 min and resolved on a polyacrylamide gel. The predicted secondary structures of each aptamer were generated by mfold. (**B**) The percent full extension was quantified for m.1.1FL (filled inverted triangle), m.1.3 (filled circle) and m.1.4 (filled square) and data points fit to one-site competition non-linear regression using GraphPad Prism 4 to calculate $IC_{50}$. HIV-1 RT was not susceptible to m.1.1FL (open triangle). (Errors represent data deviation from the fit).

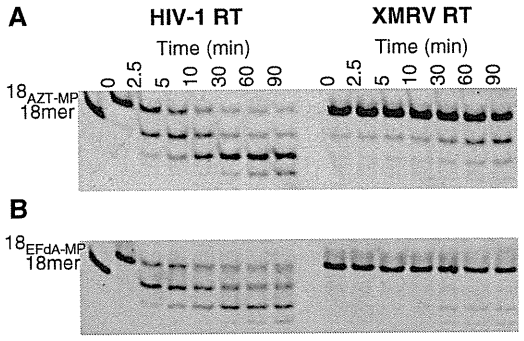


**Figure 8.** PPi-mediated unblocking of AZT-(A) and EFdA-(B) terminated DNA. About 20 nM of (**A**) AZT- or (**B**) EFdA-terminated $T_{d31}$/Cy3-$P_{d18c}$ (T/$P_{AZT\text{-}MP}$ or T/$P_{EFdA\text{-}MP}$) was incubated with HIV-1 RT (60 nM) or XMRV RT (200 nM) in the presence of 150 μM PPi and 6 mM $MgCl_2$. Aliquots of the reactions were stopped at different time points (0–90 min) and resolved on a 15% polyacrylamide–7M urea gel as described in the 'Materials and Methods' section.

## Susceptibility of mutant XMRV RTs to AZT-TP and tenofovir-DP

The HIV-1 RT mutation Q151M confers resistance to AZT by enhancing discrimination of the nucleotide analog leading to its reduced incorporation (37,66–68). Another HIV-1 RT mutation, K65R, decreases susceptibility to tenofovir (69,70). Since AZT and tenofovir are potent inhibitors of XMRV (Table 6) (54–56), we wanted to investigate whether the XMRV RT mutant equivalents of HIV Q151M and K65R (XMRV Q190M and K103R) would confer XMRV RT resistance to AZT and tenofovir. We constructed these mutant clones and tested their susceptibility to AZT and tenofovir in the same manner as wild-type XMRV RT. Interestingly, Q190M XMRV RT has a decreased susceptibility to AZT (approximately 5-fold increase in the $IC_{50}$). Similarly, the K103R XMRV RT mutant enzyme was less susceptible to tenofovir, increasing the $IC_{50}$ by at least 2-fold.

## Molecular model of XMRV RT

Given the significant sequence similarity between XMRV and MoMLV RTs, the resulting homology model of XMRV RT is highly similar to MoMLV RT (>1.5Å rms) and of excellent quality. Since the input structure of MoMLV RT did not contain the RNase H domain of the enzyme, the XMRV RT model is also missing this domain. The molecular model of the polymerase domain of XMRV RT is shown in Figure 9. An alignment of the MoMLV RT crystal structure (22) with the XMRV RT homology model highlights the few changes in the polymerase domain of XMRV RT. These are L29 (P in MoMLV), Q234 (L in MoMLV), R238 (Q in MoMLV) and N422 (D in MoMLV). From these, residue 422 is located in the nucleic acid binding cleft and may contribute to differences in the interactions with nucleic acid substrate. However, most of the differences between the gammaretroviral enzymes are in their RNase H domains and also in the first 30 N-terminal residues of the polymerase domain, for which we do not have structural

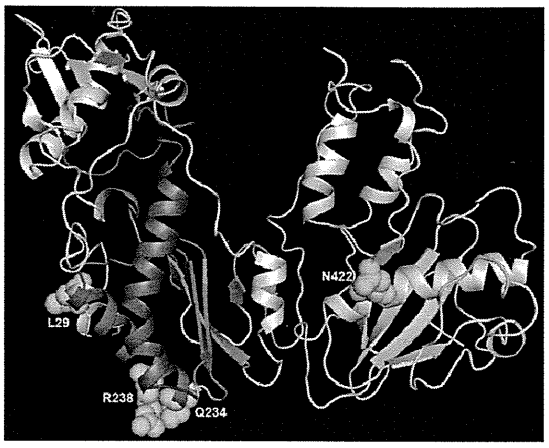


**Figure 9.** Molecular model of XMRV RT. Ribbons diagram of XMRV RT with the conserved polymerase Motifs color-coded: Motif A (green), B (brown), C (purple), D (red), E (orange) and F (blue). The residues that differ from MoMLV's polymerase domain are shown in ball and stick representation.

information since they were not included in the original crystal structure of MoMLV RT. The differences between XMRV RT and HIV-1 RT are very significant. Unlike the HIV enzyme, XMRV RT appears to be a monomer in solution. Moreover, alignment of the HIV-1 RT–DNA complex with XMRV RT based on their active sites at the palm subdomains shows that the thumb subdomain of XMRV RT would have to be repositioned to be able to accommodate nucleic acid.

## DISCUSSION

Early studies reported the presence of XMRV in stromal cells from prostate cancer patient samples and also in CFS clinical samples. Some of the subsequent studies confirmed these findings whereas several others failed to identify XMRV in prostate cancer or in CFS patients, even when same samples were used (71). It was recently reported that human sample contamination with mouse DNA can occur frequently (17,72–74). Moreover, two coauthors from this study have recently demonstrated that XMRV is the product of recombination events between two MLV proviruses, suggesting that XMRV may not be relevant to human disease (18). Nonetheless, XMRV is still an important human retrovirus and comparisons with HIV can provide valuable insights into the fundamental mechanisms of DNA polymerization, RT inhibition and drug resistance. (75).

There is high degree of sequence similarity between the XMRV and MoMLV RTs (95% amino acid identity), and much less so with HIV-1 RT. Based on gel filtration experiments we conclude that unlike HIV-1 RT, but similar to MoMLV RT, XMRV RT exists in solution primarily as a monomer. We also included comparisons with HIV-1 RT in this study as it has been extensively studied and provides an excellent frame of reference.

We report here that there are significant differences in the DNA polymerization efficiency of the three enzymes. Although the polymerase active sites of the XMRV and MoMLV enzymes are almost identical, there is a considerable decrease in the efficiency of nucleotide incorporation by XMRV RT. Most differences in sequence are at the RNase H domain and are likely to affect polymerization by changing the positioning of DNA at the polymerase active site.

We have recently solved the crystal structure of the XMRV RNase H at high resolution (1.5Å) (pdb 3P1G) (Kirby, K.A. *et al.*, submitted for publication). We observed major differences in affinity for nucleic acid that we determined with gel-mobility shift assays and with pre-steady state kinetics. SPR experiments dissected in more detail the specific defect of XMRV RT in binding DNA. Surprisingly, XMRV RT can associate very rapidly with DNA, even more so than HIV-1 RT (Figure 1 and Table 3). However, it dissociates from DNA much faster than the HIV enzyme, resulting in an overall reduced binding affinity. A possible reason for the fast association and dissociation rates of XMRV RT may be the apparent monomeric state, which might offer facile access to the nucleic acid binding cleft, although with less contacts and lower affinity than HIV-1 RT, which is a heterodimer (76,77). This high rate of XMRV RT dissociation from DNA likely contributes to the decreased processivity observed in our study, and may have consequences in the recombination rates of this virus.

Previous sequences of XMRV from prostate cancer tumors showed low variability, suggesting that the virus may have a high fidelity of replication (1,10). Our study demonstrated that HIV-1 RT and MoMLV RT incorporated mismatched nucleotides and extended past the mismatches more efficiently than XMRV RT. Pre-steady state kinetics established that the higher overall fidelity of XMRV RT over MoMLV RT is due to a lower affinity for mismatched nucleotides. When compared to HIV-1 RT, however, XMRV RT has differs in both the nucleotide binding and incorporation steps. Nonetheless, XMRV did not have higher fidelity than a related amphotropic MLV virus or HIV-1 in a cell-based assay. It is possible that the high dNTP concentration in dividing cells can suppress mismatching events. We have previously shown (39) that as nucleotide concentrations vary in different cell lines, this can affect viral susceptibility to NRTIs, and possibly in this case also incorporation of mismatched nucleotides. Additional cell-based studies using multiple cell lines and a large panel of viruses should provide a better understanding of the relation between *in vivo* and *in vitro* fidelity.

Early studies have reported susceptibility of XMRV to some antiretrovirals that have been used in the treatment of HIV infection (53–56). In those studies the compounds were tested at the virus level. To better understand the interactions of inhibitors at their RT target level we tested here the ability of these and several more compounds to block the polymerase activity of XMRV RT. We found that two TDRTIs, EFdA-TP and ENdA-TP were very potent RT inhibitors ($IC_{50}$s: 0.43 μM and 0.14 μM, respectively). Unlike other NRTIs, these compounds have a 3′ OH group and are known to efficiently inhibit HIV replication by blocking translocation (32,58,78).

Preliminary experiments demonstrated that they also block XMRV RT by the same mechanism (data not shown).

In HIV, moderate resistance to EFdA is conferred by the emergence of the M184V mutation at the conserved X position of the conserved YXDD motif of the polymerase active site. Interestingly, XMRV and MoMLV RTs already have a valine (V223) at this position. This difference is likely to contribute to the better potency of EFdA against HIV-1 RT than XMRV RT or MoMLV RT (57,58). It may also contribute to the decreased ability of XMRV RT to unblock chain-terminated primers, as was also reported for M184V HIV-1 RT (79) and to the enhanced fidelity reported here for XMRV RT, which is also reminiscent of the previously reported high fidelity of M184V HIV-1 RT (80,81). Nonetheless, despite the presence of a Val in the YMDD motif of XMRV RT we found EFdA to inhibit very efficiently replication-competent or pseudotyped XMRV, with submicromolar $EC_{50}$s (40 and 110 nM, respectively).

Previously, highly potent aptamers were selected to inhibit MoMLV RT (60). We demonstrate here that the three aptamers we tested have varying potency against XMRV RT. Aptamer m.1.1FL was the most potent inhibitor of XMRV RT and MoMLV RT in *in vitro* assays ($IC_{50}$ = 2 and 4 nM, respectively). The fact that XMRV and MoMLV RTs are inhibited by the same aptamers at comparable efficiencies suggests that the RT residues that are different in the two enzymes are not critical to the binding of the aptamer. In contrast, heterodimeric HIV-1 RT has a very different binding cleft and is not inhibited by these aptamers.

Tenofovir is an essential component of HIV therapies and is also a potent inhibitor of XMRV RT. HIV resistance to tenofovir is conferred by a single codon mutation (K65R). HIV-1 RT residue 65 is known to interact with the incoming dNTP or the activated tenofovir analog (tenofovir diphosphate) (82). K65R causes resistance to tenofovir by lowering the $k_{pol}$ for the incorporation of the inhibitor into the nascent DNA. We prepared XMRV RT with the equivalent mutation, K103R, and determined that it has decreased susceptibility to tenofovir. Hence, it is possible for XMRV to develop tenofovir resistance through the same mechanism as HIV-1 RT. HIV resistance to AZT can occur by either decreased binding/incorporation or increased excision of the chain-terminating NRTI (33,83). HIV-1 RTs containing the M41L, D67N, K70R, T215Y/F, K219E/Q mutations show enhanced removal of AZT. Our experiments show that unlike wild-type HIV-1 RT, XMRV RT is not able to excise NRTI-terminated primers. Similarly, it was previously shown that MoMLV RT is not capable of unblocking chain-terminated primers (33).

In HIV, decreased binding of AZT is conferred initially in the presence of the primary Q151M mutation, followed by secondary mutations F77L, A62V, V75I and F116Y (27,47,84). XMRV RT already differs from wild-type HIV-1 RT in the first three of these residues (P104, Q113 and L115 versus A62, V75 and F77) (Table 1). We demonstrated that introducing the primary Q→M mutation at the equivalent XMRV RT site (Q190M) resulted in an enzyme with decreased susceptibility to AZT. Hence, it appears that these residues can confer AZT resistance to XMRV by reduced incorporation of nucleotide analogs, as is the case in HIV-2 (41). At this point we do not know if introduction of as yet unknown mutations could endow XMRV RT with the ability to unblock chain-terminated nucleic acids. The details of the molecular mechanism of XMRV resistance to tenofovir and AZT are under investigation.

In conclusion, our study provides detailed biochemical analysis of the mechanisms of polymerization, inhibition, fidelity, processivity and drug resistance of XMRV RT and how it compares with the closely related enzyme MoMLV RT and the more distantly related HIV-1 RT. The findings enhance our understanding of the basic mechanisms of reverse transcription.

## SUPPLEMENTARY DATA

Supplementary Data are available at NAR Online.

## ACKNOWLEDGEMENTS

The content of this publication does not necessarily reflect the views or policies of the Department of Health Human Services, nor does mention of trade names, commercial products or organizations imply endorsement by the U.S. Government.

## FUNDING

NIH grants (AI076119, AI079801, and AI094715, to S.G.S.), (AI074389, to D.H.B.), (AI079801 to M.A.P.); NIH Bench-to-Bedside Award and the Intramural Research Program of the NIH, National Cancer Institute, Center for Cancer Research (to V.K.P); Ministry of Knowledge and Economy, Bilateral International Collaborative R&D Program, Republic of Korea; Canadian Institutes of Health Research (CIHR) and University of Missouri (to S-L.L.); amfAR Mathilde Krim Fellowship and a CIHR Fellowship (to B.M.). Funding for open access charge: NIH grants (AI076119, AI094715, AI074389, AI079801).

*Conflict of interest statement.* None declared.

## REFERENCES

1. Urisman,A., Molinaro,R.J., Fischer,N., Plummer,S.J., Casey,G., Klein,E.A., Malathi,K., Magi-Galluzzi,C., Tubbs,R.R., Ganem,D. *et al.* (2006) Identification of a novel gammaretrovirus in prostate tumors of patients homozygous for R462Q RNASEL variant. *PLoS Pathog.*, **2**, e25.
2. Malathi,K., Dong,B., Gale,M. Jr. and Silverman,R.H. (2007) Small self-RNA generated by RNase L amplifies antiviral innate immunity. *Nature*, **448**, 816–819.
3. Arnold,R.S., Makarova,N.V., Osunkoya,A.O., Suppiah,S., Scott,T.A., Johnson,N.A., Bhosle,S.M., Liotta,D., Hunter,E., Marshall,F.F. *et al.* XMRV infection in patients with prostate cancer: novel serologic assay and correlation with PCR and FISH. *Urology*, **75**, 755–761.
4. Dong,B., Kim,S., Hong,S., Das Gupta,J., Malathi,K., Klein,E.A., Ganem,D., Derisi,J.L., Chow,S.A. and Silverman,R.H. (2007) An

infectious retrovirus susceptible to an IFN antiviral pathway from human prostate tumors. *Proc Natl Acad Sci. USA*, **104**, 1655–1660.
5. Knouf,E.C., Metzger,M.J., Mitchell,P.S., Arroyo,J.D., Chevillet,J.R., Tewari,M. and Miller,A.D. (2009) Multiple integrated copies and high-level production of the human retrovirus XMRV (xenotropic murine leukemia virus-related virus) from 22Rv1 prostate carcinoma cells. *J. Virol.*, **83**, 7353–7356.
6. Schlaberg,R., Choe,D.J., Brown,K.R., Thaker,H.M. and Singh,I.R. (2009) XMRV is present in malignant prostatic epithelium and is associated with prostate cancer, especially high-grade tumors. *Proc. Natl Acad. Sci. USA*, **106**, 16351–16356.
7. Sabunciyan,S., Mandelberg,N., Rabkin,C.S., Yolken,R. and Viscidi,R. No difference in antibody titers against xenotropic MLV related virus in prostate cancer cases and cancer-free controls. *Mol. Cell. Probes.*, **25**, 134–136.
8. Verhaegh,G.W., de Jong,A.S., Smit,F.P., Jannink,S.A., Melchers,W.J. and Schalken,J.A. (2011) Prevalence of human xenotropic murine leukemia virus-related gammaretrovirus (XMRV) in Dutch prostate cancer patients. *Prostate*, **71**, 415–420.
9. Hohn,O., Krause,H., Barbarotto,P., Niederstadt,L., Beimforde,N., Denner,J., Miller,K., Kurth,R. and Bannert,N. (2009) Lack of evidence for xenotropic murine leukemia virus-related virus(XMRV) in German prostate cancer patients. *Retrovirology*, **6**, 92.
10. Lombardi,V.C., Ruscetti,F.W., Das Gupta,J., Pfost,M.A., Hagen,K.S., Peterson,D.L., Ruscetti,S.K., Bagni,R.K., Petrow-Sadowski,C., Gold,B. *et al.* (2009) Detection of an infectious retrovirus, XMRV, in blood cells of patients with chronic fatigue syndrome. *Science*, **326**, 585–589.
11. Henrich,T.J., Li,J.Z., Felsenstein,D., Kotton,C.N., Plenge,R.M., Pereyra,F., Marty,F.M., Lin,N.H., Grazioso,P., Crochiere,D.M. *et al.* (2010) Xenotropic murine leukemia virus-related virus prevalence in patients with chronic fatigue syndrome or chronic immunomodulatory conditions. *J. Infect. Dis.*, **202**, 1478–1481.
12. Erlwein,O., Kaye,S., McClure,M.O., Weber,J., Wills,G., Collier,D., Wessely,S. and Cleare,A. (2010) Failure to detect the novel retrovirus XMRV in chronic fatigue syndrome. *PLoS ONE*, **5**, e8519.
13. Groom,H.C., Boucherit,V.C., Makinson,K., Randal,E., Baptista,S., Hagan,S., Gow,J.W., Mattes,F.M., Breuer,J., Kerr,J.R. *et al.* (2010) Absence of xenotropic murine leukaemia virus-related virus in UK patients with chronic fatigue syndrome. *Retrovirology*, **7**, 10.
14. Switzer,W.M., Jia,H., Hohn,O., Zheng,H., Tang,S., Shankar,A., Bannert,N., Simmons,G., Hendry,R.M., Falkenberg,V.R. *et al.* (2010) Absence of evidence of xenotropic murine leukemia virus-related virus infection in persons with chronic fatigue syndrome and healthy controls in the United States. *Retrovirology*, **7**, 57.
15. Satterfield,B.C., Garcia,R.A., Jia,H., Tang,S., Zheng,H. and Switzer,W.M. (2011) Serologic and PCR testing of persons with chronic fatigue syndrome in the United States shows no association with xenotropic or polytropic murine leukemia virus-related viruses. *Retrovirology*, **8**, 12.
16. Menendez-Arias,L. Evidence and controversies on the role of XMRV in prostate cancer and chronic fatigue syndrome. *Rev. Med. Virol.*, **21**, 3–17.
17. Hue,S., Gray,E.R., Gall,A., Katzourakis,A., Tan,C.P., Houldcroft,C.J., McLaren,S., Pillay,D., Futreal,A., Garson,J.A. *et al.* (2010) Disease-associated XMRV sequences are consistent with laboratory contamination. *Retrovirology*, **7**, 111.
18. Paprotka,T., Delviks-Frankenberry,K.A., Cingoz,O., Martinez,A., Kung,H.J., Tepper,C.G., Hu,W.S., Fivash,M.J. Jr., Coffin,J.M. and Pathak,V.K. (2011) Recombinant origin of the retrovirus XMRV. *Science*, **333**, 97–101.
19. Singh,K., Kaushik,N., Jin,J., Madhusudanan,M. and Modak,M.J. (2000) Role of Q190 of MuLV RT in ddNTP resistance and fidelity of DNA synthesis: a molecular model of interactions with substrates. *Protein Eng.*, **13**, 635–643.
20. Telesnitsky,A. and Goff,S.P. (1993) Two defective forms of reverse transcriptase can complement to restore retroviral infectivity. *EMBO J.*, **12**, 4433–4438.
21. Georgiadis,M.M., Jessen,S.M., Ogata,C.M., Telesnitsky,A., Goff,S.P. and Hendrickson,W.A. (1995) Mechanistic implications from the structure of a catalytic fragment of Moloney murine leukemia virus reverse transcriptase. *Structure*, **3**, 879–892.
22. Das,D. and Georgiadis,M.M. (2004) The crystal structure of the monomeric reverse transcriptase from Moloney murine leukemia virus. *Structure*, **12**, 819–829.
23. Chowdhury,K., Kaushik,N., Pandey,V.N. and Modak,M.J. (1996) Elucidation of the role of Arg 110 of murine leukemia virus reverse transcriptase in the catalytic mechanism: biochemical characterization of its mutant enzymes. *Biochemistry*, **35**, 16610–16620.
24. Kaushik,N., Chowdhury,K., Pandey,V.N. and Modak,M.J. (2000) Valine of the YVDD motif of moloney murine leukemia virus reverse transcriptase: role in the fidelity of DNA synthesis. *Biochemistry*, **39**, 5155–5165.
25. Jacobo-Molina,A., Ding,J., Nanni,R.G., Clark,A.D. Jr., Lu,X., Tantillo,C., Williams,R.L., Kamer,G., Ferris,A.L., Clark,P. *et al.* (1993) Crystal structure of human immunodeficiency virus type 1 reverse transcriptase complexed with double-stranded DNA at 3.0 A resolution shows bent DNA. *Proc. Natl Acad. Sci. USA*, **90**, 6320–6324.
26. Kohlstaedt,L.A., Wang,J., Friedman,J.M., Rice,P.A. and Steitz,T.A. (1992) Crystal structure at 3.5 A resolution of HIV-1 reverse transcriptase complexed with an inhibitor. *Science*, **256**, 1783–1790.
27. Sarafianos,S.G., Marchand,B., Das,K., Himmel,D.M., Parniak,M.A., Hughes,S.H. and Arnold,E. (2009) Structure and function of HIV-1 reverse transcriptase: molecular mechanisms of polymerization and inhibition. *J. Mol. Biol.*, **385**, 693–713.
28. Singh,K., Marchand,B., Kirby,K.A., Michailidis,E. and Sarafianos,S.G. (2010) Structural aspects of drug resistance and inhibition of HIV-1 reverse transcriptase. *Viruses*, **2**, 606–638.
29. Schuckmann,M.M., Marchand,B., Hachiya,A., Kodama,E.N., Kirby,K.A., Singh,K. and Sarafianos,S.G. (2010) The N348I mutation at the connection subdomain of HIV-1 reverse transcriptase decreases binding to nevirapine. *J. Biol. Chem.*, **285**, 38700–38709.
30. Telesnitsky,A. and Goff,S.P. (1993) RNase H domain mutations affect the interaction between Moloney murine leukemia virus reverse transcriptase and its primer-template. *Proc. Natl Acad. Sci. USA*, **90**, 1276–1280.
31. Bauman,J.D., Das,K., Ho,W.C., Baweja,M., Himmel,D.M., Clark,A.D. Jr., Oren,D.A., Boyer,P.L., Hughes,S.H., Shatkin,A.J. *et al.* (2008) Crystal engineering of HIV-1 reverse transcriptase for structure-based drug design. *Nucleic Acids Res.*, **36**, 5083–5092.
32. Michailidis,E., Marchand,B., Kodama,E.N., Singh,K., Matsuoka,M., Kirby,K.A., Ryan,E.M., Sawani,A.M., Nagy,E., Ashida,N. *et al.* (2009) Mechanism of inhibition of HIV-1 reverse transcriptase by 4′-Ethynyl-2-fluoro-2′-deoxyadenosine triphosphate, a translocation-defective reverse transcriptase inhibitor. *J. Biol. Chem.*, **284**, 35681–35691.
33. Meyer,P.R., Matsuura,S.E., So,A.G. and Scott,W.A. (1998) Unblocking of chain-terminated primer by HIV-1 reverse transcriptase through a nucleotide-dependent mechanism. *Proc. Natl Acad. Sci. USA*, **95**, 13471–13476.
34. Halvas,E.K., Svarovskaia,E.S. and Pathak,V.K. (2000) Development of an in vivo assay to identify structural determinants in murine leukemia virus reverse transcriptase important for fidelity. *J Virol*, **74**, 312–319.
35. Patel,S.S., Wong,I. and Johnson,K.A. (1991) Pre-steady-state kinetic analysis of processive DNA replication including complete characterization of an exonuclease-deficient mutant. *Biochemistry*, **30**, 511–525.
36. Sarafianos,S.G., Clark,A.D. Jr., Das,K., Tuske,S., Birktoft,J.J., Ilankumaran,P., Ramesha,A.R., Sayer,J.M., Jerina,D.M., Boyer,P.L. *et al.* (2002) Structures of HIV-1 reverse transcriptase with pre- and post-translocation AZTMP-terminated DNA. *EMBO J.*, **21**, 6614–6624.
37. Tuske,S., Sarafianos,S.G., Clark,A.D. Jr., Ding,J., Naeger,L.K., White,K.L., Miller,M.D., Gibbs,C.S., Boyer,P.L., Clark,P. *et al.* (2004) Structures of HIV-1 RT-DNA complexes before and after

incorporation of the anti-AIDS drug tenofovir. *Nat. Struct. Mol. Biol.*, **11**, 469–474.
38. Sarafianos,S.G., Pandey,V.N., Kaushik,N. and Modak,M.J. (1995) Site-directed mutagenesis of arginine 72 of HIV-1 reverse transcriptase. Catalytic role and inhibitor sensitivity. *J. Biol. Chem.*, **270**, 19729–19735.
39. Hachiya,A., Kodama,E.N., Schuckmann,M.M., Kirby,K.A., Michailidis,E., Sakagami,Y., Oka,S., Singh,K. and Sarafianos,S.G. (2011) K70Q adds high-level tenofovir resistance to "Q151M complex" HIV reverse transcriptase through the enhanced discrimination mechanism. *PLoS One*, **6**, e16242.
40. Sarafianos,S.G., Das,K., Ding,J., Boyer,P.L., Hughes,S.H. and Arnold,E. (1999) Touching the heart of HIV-1 drug resistance: the fingers close down on the dNTP at the polymerase active site. *Chem. Biol.*, **6**, R137–R146.
41. Boyer,P.L., Sarafianos,S.G., Clark,P.K., Arnold,E. and Hughes,S.H. (2006) Why do HIV-1 and HIV-2 use different pathways to develop AZT resistance? *PLoS Pathog.*, **2**, e10.
42. Powell,M.D., Ghosh,M., Jacques,P.S., Howard,K.J., Le Grice,S.F. and Levin,J.G. (1997) Alanine-scanning mutations in the "primer grip" of p66 HIV-1 reverse transcriptase result in selective loss of RNA priming activity. *J. Biol. Chem.*, **272**, 13262–13269.
43. Sarafianos,S.G., Das,K., Clark,A.D. Jr., Ding,J., Boyer,P.L., Hughes,S.H. and Arnold,E. (1999) Lamivudine (3TC) resistance in HIV-1 reverse transcriptase involves steric hindrance with beta-branched amino acids. *Proc. Natl Acad. Sci. USA*, **96**, 10027–10032.
44. Boucher,C.A., Cammack,N., Schipper,P., Schuurman,R., Rouse,P., Wainberg,M.A. and Cameron,J.M. (1993) High-level resistance to (-) enantiomeric 2′-deoxy-3′-thiacytidine in vitro is due to one amino acid substitution in the catalytic site of human immunodeficiency virus type 1 reverse transcriptase. *Antimicrob. Agents Chemother.*, **37**, 2231–2234.
45. Tisdale,M., Kemp,S.D., Parry,N.R. and Larder,B.A. (1993) Rapid in vitro selection of human immunodeficiency virus type 1 resistant to 3′-thiacytidine inhibitors due to a mutation in the YMDD region of reverse transcriptase. *Proc. Natl Acad. Sci. USA*, **90**, 5653–5656.
46. Menendez-Arias,L. (2010) Molecular basis of human immunodeficiency virus drug resistance: an update. *Antiviral Res.*, **85**, 210–231.
47. Sarafianos,S.G., Das,K., Hughes,S.H. and Arnold,E. (2004) Taking aim at a moving target: designing drugs to inhibit drug-resistant HIV-1 reverse transcriptases. *Curr. Opin. Struct. Biol.*, **14**, 716–730.
48. Menendez-Arias,L. (2010) Molecular basis of human immunodeficiency virus drug resistance: an update. *Antiviral Res.*, **85**, 210–231.
49. Menendez-Arias,L. and Berkhout,B. (2008) Retroviral reverse transcription. *Virus Res.*, **134**, 1–3.
50. Shi,Q., Singh,K., Srivastava,A., Kaushik,N. and Modak,M.J. (2002) Lysine 152 of MuLV reverse transcriptase is required for the integrity of the active site. *Biochemistry*, **41**, 14831–14842.
51. Johnson,K.A. (1993) Conformational coupling in DNA polymerase fidelity. *Annu. Rev. Biochem.*, **62**, 685–713.
52. Rezende,L.F. and Prasad,V.R. (2004) Nucleoside-analog resistance mutations in HIV-1 reverse transcriptase and their influence on polymerase fidelity and viral mutation rates. *Int. J. Biochem. Cell Biol.*, **36**, 1716–1734.
53. Paprotka,T., Venkatachari,N.J., Chaipan,C., Burdick,R., Delviks-Frankenberry,K.A., Hu,W.S. and Pathak,V.K. Inhibition of xenotropic murine leukemia virus-related virus by APOBEC3 proteins and antiviral drugs. *J. Virol.*, **84**, 5719–5729.
54. Sakuma,R., Sakuma,T., Ohmine,S., Silverman,R.H. and Ikeda,Y. (2010) Xenotropic murine leukemia virus-related virus is susceptible to AZT. *Virology*, **397**, 1–6.
55. Singh,I.R., Gorzynski,J.E., Drobysheva,D., Bassit,L. and Schinazi,R.F. (2010) Raltegravir is a potent inhibitor of XMRV, a virus implicated in prostate cancer and chronic fatigue syndrome. *PLoS One*, **5**, e9948.
56. Smith,R.A., Gottlieb,G.S. and Miller,A.D. (2010) Susceptibility of the human retrovirus XMRV to antiretroviral inhibitors. *Retrovirology*, **7**, 70.
57. Kawamoto,A., Kodama,E., Sarafianos,S.G., Sakagami,Y., Kohgo,S., Kitano,K., Ashida,N., Iwai,Y., Hayakawa,H., Nakata,H. *et al.* (2008) 2′-deoxy-4′-C-ethynyl-2-halo-adenosines active against drug-resistant human immunodeficiency virus type 1 variants. *Int. J. Biochem. Cell Biol.*, **40**, 2410–2420.
58. Kodama,E.I., Kohgo,S., Kitano,K., Machida,H., Gatanaga,H., Shigeta,S., Matsuoka,M., Ohrui,H. and Mitsuya,H. (2001) 4′-Ethynyl nucleoside analogs: potent inhibitors of multidrug-resistant human immunodeficiency virus variants in vitro. *Antimicrob. Agents Chemother.*, **45**, 1539–1546.
59. Kissel,J.D., Held,D.M., Hardy,R.W. and Burke,D.H. (2007) Single-stranded DNA aptamer RT1t49 inhibits RT polymerase and RNase H functions of HIV type 1, HIV type 2, and SIVCPZ RTs. *AIDS Res. Hum. Retroviruses.*, **23**, 699–708.
60. Chen,H. and Gold,L. (1994) Selection of high-affinity RNA ligands to reverse transcriptase: inhibition of cDNA synthesis and RNase H activity. *Biochemistry*, **33**, 8746–8756.
61. Joshi,P.J., Fisher,T.S. and Prasad,V.R. (2003) Anti-HIV inhibitors based on nucleic acids: emergence of aptamers as potent antivirals. *Curr. Drug Targets Infect. Disord.*, **3**, 383–400.
62. DeStefano,J.J. and Nair,G.R. (2008) Novel aptamer inhibitors of human immunodeficiency virus reverse transcriptase. *Oligonucleotides*, **18**, 133–144.
63. DeStefano,J.J. and Cristofaro,J.V. (2006) Selection of primer-template sequences that bind human immunodeficiency virus reverse transcriptase with high affinity. *Nucleic Acids Res.*, **34**, 130–139.
64. Arion,D., Kaushik,N., McCormick,S., Borkow,G. and Parniak,M.A. (1998) Phenotypic mechanism of HIV-1 resistance to 3′-azido-3′-deoxythymidine (AZT): increased polymerization processivity and enhanced sensitivity to pyrophosphate of the mutant viral reverse transcriptase. *Biochemistry*, **37**, 15908–15917.
65. Sarafianos,S.G., Hughes,S.H. and Arnold,E. (2004) Designing anti-AIDS drugs targeting the major mechanism of HIV-1 RT resistance to nucleoside analog drugs. *Int. J. Biochem. Cell Biol.*, **36**, 1706–1715.
66. Shafer,R.W., Kozal,M.J., Winters,M.A., Iversen,A.K., Katzenstein,D.A., Ragni,M.V., Meyer,W.A. 3rd, Gupta,P., Rasheed,S., Coombs,R. *et al.* (1994) Combination therapy with zidovudine and didanosine selects for drug-resistant human immunodeficiency virus type 1 strains with unique patterns of pol gene mutations. *J. Infect. Dis.*, **169**, 722–729.
67. Shirasaka,T., Kavlick,M.F., Ueno,T., Gao,W.Y., Kojima,E., Alcaide,M.L., Chokekijchai,S., Roy,B.M., Arnold,E., Yarchoan,R. *et al.* (1995) Emergence of human immunodeficiency virus type 1 variants with resistance to multiple dideoxynucleosides in patients receiving therapy with dideoxynucleosides. *Proc. Natl Acad. Sci. USA*, **92**, 2398–2402.
68. Iversen,A.K., Shafer,R.W., Wehrly,K., Winters,M.A., Mullins,J.I., Chesebro,B. and Merigan,T.C. (1996) Multidrug-resistant human immunodeficiency virus type 1 strains resulting from combination antiretroviral therapy. *J. Virol.*, **70**, 1086–1090.
69. Winters,M.A., Shafer,R.W., Jellinger,R.A., Mamtora,G., Gingeras,T. and Merigan,T.C. (1997) Human immunodeficiency virus type 1 reverse transcriptase genotype and drug susceptibility changes in infected individuals receiving dideoxyinosine monotherapy for 1 to 2 years. *Antimicrob. Agents Chemother.*, **41**, 757–762.
70. Gu,Z., Gao,Q., Fang,H., Salomon,H., Parniak,M.A., Goldberg,E., Cameron,J. and Wainberg,M.A. (1994) Identification of a mutation at codon 65 in the IKKK motif of reverse transcriptase that encodes human immunodeficiency virus resistance to 2′,3′-dideoxycytidine and 2′,3′-dideoxy-3′-thiacytidine. *Antimicrob. Agents Chemother.*, **38**, 275–281.
71. Knox,K., Carrigan,D., Simmons,G., Teque,F., Zhou,Y., Hackett,J. Jr., Qiu,X., Luk,K.C., Schochetman,G., Knox,A. *et al.* (2011) No evidence of murine-like gammaretroviruses in CFS patients previously identified as XMRV-infected. *Science*.
72. Oakes,B., Tai,A.K., Cingoz,O., Henefield,M.H., Levine,S., Coffin,J.M. and Huber,B.T. (2010) Contamination of human DNA samples with mouse DNA can lead to false detection of XMRV-like sequences. *Retrovirology*, **7**, 109.
73. Robinson,M.J., Erlwein,O.W., Kaye,S., Weber,J., Cingoz,O., Patel,A., Walker,M.M., Kim,W.J., Uiprasertkul,M., Coffin,J.M.

*et al.* (2010) Mouse DNA contamination in human tissue tested for XMRV. *Retrovirology*, **7**, 108.
74. Sato,E., Furuta,R.A. and Miyazawa,T. (2010) An endogenous murine leukemia viral genome contaminant in a commercial RT-PCR kit is amplified using standard primers for XMRV. *Retrovirology*, **7**, 110.
75. Coffin,J.M. and Stoye,J.P. (2009) Virology. A new virus for old diseases? *Science*, **326**, 530–531.
76. Huang,H., Chopra,R., Verdine,G.L. and Harrison,S.C. (1998) Structure of a covalently trapped catalytic complex of HIV-1 reverse transcriptase: implications for drug resistance. *Science*, **282**, 1669–1675.
77. Sarafianos,S.G., Das,K., Tantillo,C., Clark,A.D. Jr., Ding,J., Whitcomb,J.M., Boyer,P.L., Hughes,S.H. and Arnold,E. (2001) Crystal structure of HIV-1 reverse transcriptase in complex with a polypurine tract RNA:DNA. *EMBO J.*, **20**, 1449–1461.
78. Kirby,K.A., Singh,K., Michailidis,E., Marchand,B., Kodama,E.N., Ashida,N., Mitsuya,H., Parniak,M.A. and Sarafianos,S.G. The sugar ring conformation of 4′-ethynyl-2-fluoro-2′-deoxyadenosine and its recognition by the polymerase active site of hiv reverse transcriptase. *Cell Mol. Biol.*, **57**, 40–46.
79. Gotte,M., Arion,D., Parniak,M.A. and Wainberg,M.A. (2000) The M184V mutation in the reverse transcriptase of human immunodeficiency virus type 1 impairs rescue of chain-terminated DNA synthesis. *J. Virol.*, **74**, 3579–3585.
80. Wainberg,M.A., Drosopoulos,W.C., Salomon,H., Hsu,M., Borkow,G., Parniak,M., Gu,Z., Song,Q., Manne,J., Islam,S. *et al.* (1996) Enhanced fidelity of 3TC-selected mutant HIV-1 reverse transcriptase. *Science*, **271**, 1282–1285.
81. Pandey,V.N., Kaushik,N., Rege,N., Sarafianos,S.G., Yadav,P.N. and Modak,M.J. (1996) Role of methionine 184 of human immunodeficiency virus type-1 reverse transcriptase in the polymerase function and fidelity of DNA synthesis. *Biochemistry*, **35**, 2168–2179.
82. Das,K., Bandwar,R.P., White,K.L., Feng,J.Y., Sarafianos,S.G., Tuske,S., Tu,X., Clark,A.D. Jr., Boyer,P.L., Hou,X. *et al.* (2009) Structural basis for the role of the K65R mutation in HIV-1 reverse transcriptase polymerization, excision antagonism, and tenofovir resistance. *J. Biol. Chem.*, **284**, 35092–35100.
83. Meyer,P.R., Matsuura,S.E., Mian,A.M., So,A.G. and Scott,W.A. (1999) A mechanism of AZT resistance: an increase in nucleotide-dependent primer unblocking by mutant HIV-1 reverse transcriptase. *Mol. Cell.*, **4**, 35–43.
84. Ueno,T., Shirasaka,T. and Mitsuya,H. (1995) Enzymatic characterization of human immunodeficiency virus type 1 reverse transcriptase resistant to multiple 2′,3′-dideoxynucleoside 5′-triphosphates. *J. Biol. Chem.*, **270**, 23605–23611.
85. Rhee,S.Y., Gonzales,M.J., Kantor,R., Betts,B.J., Ravela,J. and Shafer,R.W. (2003) Human immunodeficiency virus reverse transcriptase and protease sequence database. *Nucleic Acids Res.*, **31**, 298–303.

Published in final edited form as:
*Cell Mol Biol (Noisy-le-grand)*. ; 58(1): 187–195.

# EFFECT OF TRANSLOCATION DEFECTIVE REVERSE TRANSCRIPTASE INHIBITORS ON THE ACTIVITY OF N348I, A CONNECTION SUBDOMAIN DRUG RESISTANT HIV-1 REVERSE TRANSCRIPTASE MUTANT

**E. MICHAILIDIS**[1], **K. SINGH**[1], **E.M. RYAN**[1], **A. HACHIYA**[1], **Y.T. ONG**[1], **K.A. KIRBY**[1], **B. MARCHAND**[1], **E.N. KODAMA**[2], **H. MITSUYA**[3], **M.A. PARNIAK**[4], and **S.G. SARAFIANOS**[1,5,*]

[1]Christopher S. Bond Life Sciences Center and Department of Molecular Microbiology & Immunology, School of Medicine, University of Missouri, Columbia, MO 65211, USA

[2]Division of Emerging Infectious Diseases, Tohoku University School of Medicine, Sendai 980-8575, Japan

[3]Department of Hematology and Infectious Diseases, Kumamoto University, Kumamoto 860-8556, Japan & Experimental Retrovirology Section, HIV/AIDS Malignancy Branch, NIH, Bethesda, MD 20892, USA

[4]Department of Molecular Genetics & Biochemistry University of Pittsburgh School of Medicine, Pittsburgh, PA 15261, USA

[5]Department of Biochemistry, University of Missouri, Columbia, MO 65211, USA

## Abstract

4′-ethynyl-2-fluoro-2′-deoxyadenosine (EFdA) is a highly potent inhibitor of HIV-1 reverse transcriptase (RT). We have previously shown that its exceptional antiviral activity stems from a unique mechanism of action that is based primarily on blocking translocation of RT; therefore we named EFdA a Translocation Defective RT Inhibitor (TDRTI). The N348I mutation at the connection subdomain (CS) of HIV-1 RT confers clinically significant resistance to both nucleoside (NRTIs) and non-nucleoside RT inhibitors (NNRTIs). In this study we tested EFdA-triphosphate (TP) together with a related compound, ENdA-TP (4′-ethynyl-2-amino-2′-deoxyadenosine triphosphate) against HIV-1 RTs that carry clinically relevant drug resistance mutations: N348I, D67N/K70R/L210Q/T215F, D67N/K70R/L210Q/T215F/N348I, and A62V/V75I/F77L/F116Y/Q151M. We demonstrate that these enzymes remain susceptible to TDRTIs. Similar to WT RT, the N348I RT is inhibited by EFdA mainly at the point of incorporation through decreased translocation. In addition, the N348I substitution decreases the RNase H cleavage of DNA terminated with EFdA-MP ($T/P_{EFdA\text{-}MP}$). Moreover, N348I RT unblocks EFdA-terminated primers with similar efficiency as the WT enzyme, and further enhances EFdA unblocking in the background of AZT-resistance mutations. This study provides biochemical insights into the mechanism of inhibition of N348I RT by TDRTIs and highlights the excellent efficacy of this class of inhibitors against WT and drug-resistant HIV-1 RTs.

### Keywords

EFdA; ENdA; N348I; Translocation Defective Reverse Transcriptase Inhibitors; Reverse Transcriptase; HIV-1; Antivirals

*Correspond to: sarafianoss@missouri.edu, Phone: 573-882-4338, Fax: 573-884-9676.

## INTRODUCTION

Human immunodeficiency virus type 1 reverse transcriptase (HIV-1 RT) is a key enzyme that converts single-stranded genomic RNA into double-stranded DNA, which in turn is transported to the nucleus and integrated into the host cell genome. The HIV-1 RT catalyzes both the RNA- and DNA-dependent DNA polymerase, and RNase H activities (11). The functional form of HIV-1 RT is a heterodimer consisting of p66 and p51 polypeptides (16). The p66 subunit has both enzymatic activities and includes the polymerase and the RNase H domains. The polymerase domain consists of the fingers, palm and thumb subdomains which are analogous to a right hand connected to the RNase H domain through the connection subdomain (42) (Fig. 1).

The p51 subunit lacks the RNase H domain and has been proposed to play a structural role (42), although recent work from our laboratory has also shown that mutations in the p51 subunit affect the polymerase and RNase H enzymatic functions of RT (38).

Highly active antiretroviral therapies (HAART) have been very effective in suppressing viral loads and having a significant impact on the life expectancy of HIV patients. Key components of HAART are drugs that target HIV RT. The two classes of RT inhibitors currently used in the clinic are nucleoside/nucleotide RT inhibitors (NRTI) and non-nucleoside RT inhibitors (NNRTI). NRTIs inhibit RT by acting as chain-terminators after they are incorporated into the nascent DNA chain. NNRTIs act non-competitively by binding to a hydrophobic pocket adjacent to, but distinct from the polymerase active site of RT and by imposing rigidity to the movements of thumb subdomain required for efficient polymerase function (20, 22, 35, 37, 39, 41).

Despite the phenomenal success of HAART regimens, continuous use of antivirals leads to the emergence of viruses that are resistant to all known anti-AIDS drugs. The mutations associated with NNRTI resistance are generally located at the NNRTI binding pocket (NNIBP). However, the mutations that cause resistance to NRTIs have been noted to be scattered in the polymerase domain (22, 39). While most NNRTI and NRTI resistance mutations are at the palm and fingers subdomains of HIV-1 RT, it has recently been shown that some mutations associated with NNRTI and NRTI resistance are at the connection and RNase H regions of RT (6, 8, 13, 15, 17, 29, 43). The most significant of these mutations is N348I, which confers moderate resistance to both NRTIs and NNRTIs, and is present in a significant number of clinical isolates, especially in the presence of other NRTI mutations.

In light of the new emerging drug resistance mutations, it is essential to identify inhibitors that are very potent and effective against viral strains that are resistant to all approved therapeutics. One such inhibitor is 4′-ethynyl-2-fluoro-2′-deoxyadenosine triphosphate (EFdA-TP) (18, 19). We have recently reported the mechanism of HIV inhibition by EFdA (26). In contrast to other approved NRTIs, which have a modification at 3′OH, EFdA contains a 3′OH moiety and blocks DNA synthesis by locking the primer terminus at the pre-translocation site of HIV-1 RT. In addition to EFdA, we have recently shown that ENdA also inhibits HIV RT potently acting as a TDRTI (data not shown).

Recently, using transient-state kinetic experiments we established the mechanism of NNRTI resistance of HIV-1 RT containing the N348I mutation at the connection subdomain of the enzyme (38). We showed that the resistance to the NNRTI nevirapine (NEV) is primarily the result of changes distant from the NNRTI binding pocket, which decrease inhibitor binding (increase $K_{d\text{-}NVP}$) by primarily decreasing the association rate of the inhibitor ($k_{on\text{-}NVP}$). Moreover, the N348I mutation increased nucleic acid binding affinity, enhanced processivity and lowered the catalytic turnover rate of the natural substrate. In this study we

determine the ability of TDRTIs to block reverse transcription by the multi-drug resistant N348I HIV-1 RT as well as other NRTI resistant RTs, D67N/K70R/L210Q/T215F (resistant to AZT by the excision mechanism) D67N/K70R/L210Q/T215F/N348I, and A62V/V75I/F77L/F116Y/Q151M (multidrug resistant to AZT and dideoxynucleotide RT inhibitors).

## MATERIALS AND METHODS

### Enzymes and Nucleic acids

The RT genes coding for p66 and p51 subunits of BH10 HIV-1 were cloned in the pETDuet-1 vector (Novagen) using restriction sites *NcoI* and *SacI* for the p51 subunit, and *SacII* and *AvrII* for the p66 subunit (2, 38). The sequences coding for a hexa-histidine tag and the 3C protease recognition sequence were added at the N-terminus of the p51 subunit. RT was expressed in BL21 (Invitrogen) and purified by nickel affinity chromatography and monoQ anion exchange chromatography (33). Oligonucleotides used in this study were chemically synthesized and purchased from Integrated DNA Technologies (Coralville, IA). Sequences of the DNA substrates are shown in Table 1. Deoxynucleotide triphosphates and dideoxynucleotide triphosphates were purchased from Fermentas (Glen Burnie, MD). EFdA and ENdA were synthesized by Yamasa Corporation (Chiba, Japan) as described before (30). Using EFdA and ENdA as starting material the triphosphate forms EFdA-TP and ENdA-TP were synthesized by TriLink BioTechnologies (San Diego, CA). Concentrations of nucleotides, EFdA-TP and ENdA-TP were calculated spectrophotometrically on the basis of absorption at 260 nm and their extinction coefficients. All nucleotides were treated with inorganic pyrophosphatase (Roche Diagnostics) as described previously (24) to remove traces of PPi contamination that might interfere with the rescue assay.

### Primer extension assays

**Inhibition of HIV-1 RT by TDRTIs**—DNA template ($T_{d31}$) was annealed to 5′-Cy3 labeled DNA primer ($P_{d18}$). To monitor primer extension, the $T_{d31}$/5′Cy3-$P_{d18}$ hybrid (20 nM) was incubated at 37°C with WT or drug-resistant HIV-1 RTs (20 nM) in a buffer containing 50 mM Tris (pH 7.8) and 50 mM NaCl (RT buffer). Varying amounts of EFdA-TP or ENdA-TP were added and the reactions were initiated by the addition of 6 mM $MgCl_2$ to a final volume of 20 μl. All dNTPs were present at a final concentration of 1 μM. The reactions were terminated after 15 minutes by adding equal volume of 100% formamide containing traces of bromophenol blue. The products were resolved on a 15% polyacrylamide 7 M urea gel. In this and in subsequent assays, the gels were scanned with a PhosphorImager (FujiFilm FLA 5000), the bands for fully extended product were quantified using Multi Gauge (FujiFilm) and results were plotted using one site competition equation on GraphPad Prism 4 to determine the $IC_{50}$ for EFdA-TP and ENdA-TP.

**Site-specific $Fe^{2+}$ Footprinting Assay**—Site-specific $Fe^{2+}$ footprints were monitored on 5′-Cy3-labeled DNA templates. 100 nM of 5′Cy3-$T_{d43}$/$P_{d20}$ was incubated with 600 nM WT or N348I RT in a buffer containing 120 mM sodium cacodylate (pH 7), 20 mM NaCl, 6 mM $MgCl_2$, and either of 5 μM ddATP or 1 μM EFdA-TP, to allow quantitative chain-termination. Prior to the treatment with $Fe^{2+}$, complexes were pre-incubated for 7 min with increasing concentrations of the next incoming nucleotide (dTTP). The complexes were treated with ammonium iron sulfate (1 mM) as previously described (21). This reaction relies on autoxidation of $Fe^{2+}$ (3) to create a local concentration of hydroxyl radical which cleaves the DNA at the nucleotide closest to the $Fe^{2+}$ specifically bound to the RNase H active site.

**ATP-dependent Excision and Rescue assay**—20 nM of purified $T_{d31}$/$P_{d18\text{-}EFdA\text{-}MP}$ or $T_{r31}$/$P_{d18\text{-}EFdA\text{-}MP}$ were incubated with 60 nM WT, N348I, D67N/K70R/L210Q/T215F

or D67N/K70R/L210Q/T215F/N348I RT in the presence of 3.5 mM ATP, 100 μM dATP, 0.5 μM dTTP, and 10 μM ddGTP in RT buffer and 10 mM $MgCl_2$. Aliquots of the reaction were stopped at different time points (0–90 min) and analyzed as described above.

**RNase H Assays—**RNase H assays were performed by incubating the RNA/DNA duplex5′Cy3-$T_{r35}/P_{d25}$ or 5′Cy3-$T_{r35}/P_{d25\text{-}ddAMP}$ or 5′Cy3-$T_{r35}/P_{d25\text{-}EFdA\text{-}MP}$ (50 nM) with WT or N348I RT (50 nM) in RT buffer at 37 °C with $MgCl_2$ (6 mM). Reactions were quenched after incubation (1–5 min) with equal volumes of formamide containing trace amounts of bromophenol blue. Reaction products were analyzed as before. The primary RNase H cleavage product is mainly 18 nucleotides from the 3′-end of the DNA primer (18 nucleotides), and the secondary cleavage product is mainly 12 nucleotides from the 3′-end of the primer (12 nucleotides) as reported previously (10, 12, 38).

# RESULTS

The inhibitors used here to characterize the susceptibility of N348I to various drugs are adenosine analogs. The structures of these analogs are shown in Fig. 2. The normal deoxynucleotide dA is shown in Fig. 2A. EFdA and ENdA are shown in Figs. 2B and 2C, respectively. It can be seen in these figures that unlike other anti-HIV NRTIs both EFdA and ENdA have a 3′OH. These compounds also contain an ethynyl group at the 4′ position. EFdA and ENdA differ in their substitutions at the 2 position of the purine ring. EFdA at this position has fluorine whereas ENdA has an amino group.

## Inhibition of WT and N348I mutant of HIV-1 RT

The inhibition of WT, N348I, D67N/K70R/L210Q/T215F, D67N/K70R/L210Q/T215F/N348I mutants of HIV-1 RT by EFdA-TP and ENdA-TP was assessed by a primer extension assay. As shown in Fig. 3A–3D, EFdA-TP and ENdA-TP suppressed RT-catalyzed DNA synthesis in a dose-dependent manner. The $IC_{50}$ values for both analogs are shown in Table 2. N348I, D67N/K70R/L210Q/T215F and D67N/K70R/L210Q/T215F/N348I RTs were inhibited by EFdA-TP and ENdA-TP with similar efficiency compared to the WT enzyme. In addition, another mutant HIV-1 RT (A62V/V75I/F77L/F116Y/Q151M) was included in drug susceptibility assays (Fig. 3E).

We have previously shown that EFdA inhibits DNA synthesis at the point of incorporation. Thus, we examined here the stopping patterns after incorporation products of the primer extension assay for the stopping patterns (Fig. 3). The primer synthesis shown in Fig. 3 clearly demonstrates that the stopping pattern follows the incorporation of adenosine analogs. Three distinct bands at positions 1, 6 and 10 indicate that both analogs inhibit RT mainly at the point of incorporation. Therefore, these compounds act primarily as obligate chain terminators. There is also an additional band at position 7, suggesting that in some instances EFdA may allow addition of one nucleotide after its incorporation, thus acting as a delayed chain terminator (Fig. 3). This type of inhibition is far less common and is sequence-dependent. These finding agrees with our previous studies on WT RT (26).

## Effect of EFdA-MP on Translocation of WT and N348I mutant of HIV-1 RT

The connection subdomain mutation N348I has been related to the altered DNA binding affinity and processivity of the mutant enzyme compared to the WT RT (4, 38). Since EFdA is a TDRTI and its incorporation is assumed to affect the translocation and thereby DNA binding and processivity, we investigated the translocation of EFdA-containing template-primers using the hydroxyl radical site-specific footprinting assay (21). The results of the footprinting assay shown in Fig. 4 demonstrate that the presence of EFdA-MP at the 3′ end of the DNA primer blocks translocation and prevents incorporation of the next incoming

dNTP. Therefore, similar to WT RT, the mutant N348I RT is also inhibited by EFdA-TP *via* the same mechanism.

### Effect of EFdA-MP on RNase H activity of WT and N348I RTs

The template/primers containing EFdA-MP, ddAMP, or without inhibitor incorporated at the 3′ end of the primer were used in RNase H assays with WT and N348I RTs in a time dependent manner. As previously noted, Fig. 5 shows that N348I mutant RT has decreased RNase H activity for all substrates used in this assay. The RNase H assays carried out in presence of T/P trap showed the disappearance of the secondary cuts for both enzymes used here. This is likely due to a defect in translocation that EFdA imposes on the enzyme. Interestingly, the primary cut of EFdA-terminated primers is a single band when the T/P has EFdA, but not ddA at the 3′ primer terminus. Moreover, the RNA cleavage of $T_{r35}$/$P_{d25-EFdA-MP}$ was less than that of $T_{r35}$/$P_{d25-ddAMP}$ or $T_{r35}$/$P_{d25}$ possibly because of less favorable positioning at the RNase H of T/P with EFdA at the 3′ terminus.

### ATP-dependent unblocking of EFdA-MP terminated primers by WT and N348I RTs

Since EFdA-MP-terminated primers bind predominantly in a pre-translocation mode we expected that EFdA-MP will be efficiently unblocked by both WT and N348I RTs. The ATP-dependent excision and subsequent rescue of EFdA-MP primers is shown in Fig. 6. The bands marked as 'Rescued Primer" have comparable product for the WT and N348I mutant enzyme for both DNA (Fig. 6A) and RNA (Fig. 6B) templates suggesting that resistance mutant N348I does not have any significant effect on the unblocking of EFdA-MP containing primers (RNA *vs.* DNA) (Fig. 6). However, the N348I mutation in the background of AZT resistance mutations D67N, K70R, L210Q and T215F showed a 2-fold increase in unblocking EFdA-MP containing primers both with DNA and RNA templates (Fig. 6).

## DISCUSSION

There are currently more than 20 antiretrovirals that have been approved by the US Food and Drug Administration for the treatment of HIV infection. They fall into four categories, targeting HIV RT, protease, integrase, the entry step, and the fusion of the viral and cell membranes. RT inhibitors are either NRTIs or NNRTIs. The NRTIs such zidovudine (AZT) and lamivudine compete with the natural substrates and get incorporated into the nascent DNA chain, blocking further polymerization because they lack a 3′OH group required for DNA synthesis. NNRTIs such as nevirapine and efavirenz inhibit the polymerase activity of RT by binding at a hydrophobic pocket nearly 10 Å away from the polymerase active site (Fig. 1). This pocket is created after the binding of NNRTIs. The highly active antiretroviral therapy (HAART) introduced in the mid-90s contains the combination of antivirals (generally a protease inhibitor and two NRTIs or an NNRTI and two NRTIs) targets the replication of the resistant virus.

Extended or incomplete treatments with antiretrovirals result in the emergence of drug resistance mutations. In the case of drugs that target RT, most of the resistance mutations were found to be present in the polymerase domain of RT. These resistance mutations against NRTIs function primarily with two mechanisms: (i) they reduce the binding affinity/ incorporation of NRTI (34, 40) or (ii) enhance the selective excision of incorporated NRTI from a chain-terminated primer terminus (9, 23–25, 36). The resistance against NNRTIs is primarily through the mutations that reduce the binding affinity of NNRTIs (7, 31, 32, 35).

Recent studies showed that connection subdomain mutations can confer resistance to NRTIs. Nikolenko et al. suggested that some of these mutations increase AZT resistance by

reducing template RNA degradation, thereby preserving the RNA template and providing additional time for RT to excise AZT monophosphate (27, 28). Hachiya et al., (13) as well as another research group (43) identified a clinical isolate with phenotypic resistance to nevirapine (NVP) in the absence of known NNRTI mutations. This resistance was shown to be caused by N348I, a mutation at the connection subdomain of HIV-1 RT. This mutation is not a polymorphism, as it exists in more than 10% of drug-treated, but not drug-naïve HIV patients. The connection subdomain mutation N348I has been related to the altered DNA binding affinity and processivity of the mutant enzyme compared to the WT RT (4, 38). Ehteshami et al. showed that N348I enhances resistance to AZT through both RNase H-dependent and -independent mechanisms (10). Since EFdA is a TDRTI and its incorporation is assumed to affect the translocation and thereby DNA binding and processivity, we investigated the susceptibility of two highly potent antiretrovirals EFdA and ENdA.

We report that both EFdA-TP and ENdA-TP are very potent inhibitors of N348I, D67N/K70R/L210Q/T215F, D67N/K70R/L210Q/T215F/N348I, and A62V/V75I/F77L/F116Y/Q151M RTs. They inhibit RT primarily at the point of incorporation and since they prevent enzyme translocation they both belong to the TDRTI class of NRTIs. The D67N/K70R/L210Q/T215F set of mutations are the classical thymidine-associated mutations (TAMs), which are known to cause resistance to AZT by enhancing excision of AZT-terminated primers (1, 5, 23). The A62V/V75I/F77L/F116Y/Q151M set of mutations is known as the "Q151M" complex RT, and has been known as a multidrug-resistance mutation, since the latter mutations are known to be involved in resistant variants with reduced susceptibility to dideoxynucleotides and to AZT. Unlike D67N/K70R/L210Q/T215F RT, the Q151M complex decreases susceptibility to NRTIs by decreasing incorporation efficiency of the inhibitors rather than increasing excision and unblocking of chain-terminated primers (14). Finally, N348I is known to cause resistance to both NRTIs and NNRTIs. Hence, collectively, these mutants represent all mechanisms by which RT becomes resistant to available antivirals. Importantly, we find that they are all susceptible to the EFdA and ENdA TDRTIs. Hence, this new class of RT inhibitors should be able to efficiently block viruses that carry clinically relevant mutations, including the new connection domain mutation N348I.

## Acknowledgments

This work was supported by the Ministry of Knowledge and Economy, Bilateral International Collaborative Research and Development Program, Republic of Korea, National Institutes of Health Grants AI076119, AI074389, and AI100890 (to S. G. S.) and AI079801 (to M.A.P.).

## Abbreviations

| | |
|---|---|
| **EFdA** | 4′-ethynyl-2-fluoro-2′-deoxyadenosine |
| **ENdA** | 4′-ethynyl-2-amino-2′-deoxyadenosine |
| **NRTI** | Nucleoside reverse transcriptase inhibitor |
| **RT** | Reverse transcriptase |
| **T/P$_{EFdA}$** | Template/Primer terminated with 4′-ethynyl-2-fluoro-2′-deoxyadenosine |
| **TDRTI** | Translocation defective reverse transcriptase inhibitor |
| **WT** | wild-type |

## References


1. Arion D, Kaushik N, McCormick S, Borkow G, Parniak MA. Phenotypic mechanism of HIV-1 resistance to 3′-azido-3′-deoxythymidine AZT: increased polymerization processivity and enhanced sensitivity to pyrophosphate of the mutant viral reverse transcriptase. Biochemistry. 1998; 37:15908–15917. [PubMed: 9843396]
2. Bauman JD, Das K, Ho WC, Baweja M, Himmel DM, Clark AD Jr, Oren DA, Boyer PL, Hughes SH, Shatkin AJ, Arnold E. Crystal engineering of HIV-1 reverse transcriptase for structure-based drug design. Nucleic Acids Res. 2008; 36:5083–5092. [PubMed: 18676450]
3. Biaglow JE, Kachur AV. The generation of hydroxyl radicals in the reaction of molecular oxygen with polyphosphate complexes of ferrous ion. Radiat Res. 1997; 148:181–187. [PubMed: 9254738]
4. Biondi MJ, Beilhartz GL, McCormick S, Gotte M. N348I in HIV-1 reverse transcriptase can counteract the nevirapine-mediated bias toward RNase H cleavage during plus-strand initiation. J Biol Chem. 285:26966–26975. [PubMed: 20530477]
5. Boyer PL, Sarafianos SG, Arnold E, Hughes SH. Selective excision of AZTMP by drug-resistant human immunodeficiency virus reverse transcriptase. J Virol. 2001; 75:4832–4842. [PubMed: 11312355]
6. Brehm JH, Koontz D, Meteer JD, Pathak V, Sluis-Cremer N, Mellors JW. Selection of mutations in the connection and RNase H domains of human immunodeficiency virus type 1 reverse transcriptase that increase resistance to 3′-azido-3′-dideoxythymidine. J Virol. 2007; 81:7852–7859. [PubMed: 17507476]
7. Das K, Ding J, Hsiou Y, Clark AD Jr, Moereels H, Koymans L, Andries K, Pauwels R, Janssen PA, Boyer PL, Clark P, Smith RH Jr, Kroeger Smith MB, Michejda CJ, Hughes SH, Arnold E. Crystal structures of 8-Cl and 9-Cl TIBO complexed with wild-type HIV-1 RT and 8-Cl TIBO complexed with the Tyr181Cys HIV-1 RT drug-resistant mutant. J Mol Biol. 1996; 264:1085–1100. [PubMed: 9000632]
8. Delviks-Frankenberry KA, Nikolenko GN, Barr R, Pathak VK. Mutations in human immunodeficiency virus type 1 RNase H primer grip enhance 3′-azido-3′-deoxythymidine resistance. J Virol. 2007; 81:6837–6845. [PubMed: 17428874]
9. Dharmasena S, Pongracz Z, Arnold E, Sarafianos SG, Parniak MA. 3′-Azido-3′-deoxythymidine-(5′)-tetraphospho-(5′)-adenosine, the product of ATP-mediated excision of chain-terminating AZTMP, is a potent chain-terminating substrate for HIV-1 reverse transcriptase. Biochemistry. 2007; 46:828–836. [PubMed: 17223704]
10. Ehteshami M, Beilhartz GL, Scarth BJ, Tchesnokov EP, McCormick S, Wynhoven B, Harrigan PR, Gotte M. Connection domain mutations N348I and A360V in HIV-1 reverse transcriptase enhance resistance to 3′-azido-3′-deoxythymidine through both RNase H-dependent and -independent mechanisms. J Biol Chem. 2008; 283:22222–22232. [PubMed: 18547911]
11. Goff SP. Retroviral reverse transcriptase: synthesis, structure, and function. J Acquir Immune Defic Syndr. 1990; 3:817–831. [PubMed: 1694894]
12. Gotte M, Rausch JW, Marchand B, Sarafianos S, Le Grice SF. Reverse transcriptase in motion: conformational dynamics of enzyme-substrate interactions. Biochim Biophys Acta. 1804:1202–1212. [PubMed: 19665597]
13. Hachiya A, Kodama EN, Sarafianos SG, Schuckmann MM, Sakagami Y, Matsuoka M, Takiguchi M, Gatanaga H, Oka S. Amino acid mutation N348I in the connection subdomain of human immunodeficiency virus type 1 reverse transcriptase confers multiclass resistance to nucleoside and nonnucleoside reverse transcriptase inhibitors. J Virol. 2008; 82:3261–3270. [PubMed: 18216099]
14. Hachiya A, Kodama EN, Schuckmann MM, Kirby KA, Michailidis E, Sakagami Y, Oka S, Singh K, Sarafianos SG. K70Q adds high-level tenofovir resistance to "Q151M complex" HIV reverse transcriptase through the enhanced discrimination mechanism. PloS one. 2011; 6:e16242. [PubMed: 21249155]
15. Hachiya A, Shimane K, Sarafianos SG, Kodama EN, Sakagami Y, Negishi F, Koizumi H, Gatanaga H, Matsuoka M, Takiguchi M, Oka S. Clinical relevance of substitutions in the connection subdomain and RNase H domain of HIV-1 reverse transcriptase from a cohort of antiretroviral treatment-naive patients. Antiviral Res. 2009; 82:115–121. [PubMed: 19428602]

16. Jacobo-Molina A, Ding J, Nanni RG, Clark AD Jr, Lu X, Tantillo C, Williams RL, Kamer G, Ferris AL, Clark P, et al. Crystal structure of human immunodeficiency virus type 1 reverse transcriptase complexed with double-stranded DNA at 3.0 A resolution shows bent DNA. Proceedings of the National Academy of Sciences of the United States of America. 1993; 90:6320–6324. [PubMed: 7687065]
17. Julias JG, McWilliams MJ, Sarafianos SG, Alvord WG, Arnold E, Hughes SH. Mutation of amino acids in the connection domain of human immunodeficiency virus type 1 reverse transcriptase that contact the template-primer affects RNase H activity. J Virol. 2003; 77:8548–8554. [PubMed: 12857924]
18. Kawamoto A, Kodama E, Sarafianos SG, Sakagami Y, Kohgo S, Kitano K, Ashida N, Iwai Y, Hayakawa H, Nakata H, Mitsuya H, Arnold E, Matsuoka M. 2′-deoxy-4′-C-ethynyl-2-halo-adenosines active against drug-resistant human immunodeficiency virus type 1 variants. Int J Biochem Cell Biol. 2008; 40:2410–2420. [PubMed: 18487070]
19. Kodama EI, Kohgo S, Kitano K, Machida H, Gatanaga H, Shigeta S, Matsuoka M, Ohrui H, Mitsuya H. 4′-Ethynyl nucleoside analogs: potent inhibitors of multidrug-resistant human immunodeficiency virus variants in vitro. Antimicrob Agents Chemother. 2001; 45:1539–1546. [PubMed: 11302824]
20. Kohlstaedt LA, Wang J, Friedman JM, Rice PA, Steitz TA. Crystal structure at 3.5 A resolution of HIV-1 reverse transcriptase complexed with an inhibitor. Science. 1992; 256:1783–1790. [PubMed: 1377403]
21. Marchand B, Gotte M. Site-specific footprinting reveals differences in the translocation status of HIV-1 reverse transcriptase. Implications for polymerase translocation and drug resistance. J Biol Chem. 2003; 278:35362–35372. [PubMed: 12819205]
22. Menendez-Arias L, Berkhout B. Retroviral reverse transcription. Virus Res. 2008; 134:1–3. [PubMed: 18299161]
23. Meyer PR, Matsuura SE, Mian AM, So AG, Scott WA. A mechanism of AZT resistance: an increase in nucleotide-dependent primer unblocking by mutant HIV-1 reverse transcriptase. Mol Cell. 1999; 4:35–43. [PubMed: 10445025]
24. Meyer PR, Matsuura SE, So AG, Scott WA. Unblocking of chain-terminated primer by HIV-1 reverse transcriptase through a nucleotide-dependent mechanism. Proceedings of the National Academy of Sciences of the United States of America. 1998; 95:13471–13476. [PubMed: 9811824]
25. Meyer PR, Matsuura SE, Tolun AA, Pfeifer I, So AG, Mellors JW, Scott WA. Effects of specific zidovudine resistance mutations and substrate structure on nucleotide-dependent primer unblocking by human immunodeficiency virus type 1 reverse transcriptase. Antimicrob Agents Chemother. 2002; 46:1540–1545. [PubMed: 11959594]
26. Michailidis E, Marchand B, Kodama EN, Singh K, Matsuoka M, Kirby KA, Ryan EM, Sawani AM, Nagy E, Ashida N, Mitsuya H, Parniak MA, Sarafianos SG. Mechanism of inhibition of HIV-1 reverse transcriptase by 4′-Ethynyl-2-fluoro-2′-deoxyadenosine triphosphate, a translocation-defective reverse transcriptase inhibitor. J Biol Chem. 2009; 284:35681–35691. [PubMed: 19837673]
27. Nikolenko GN, Delviks-Frankenberry KA, Palmer S, Maldarelli F, Fivash MJ Jr, Coffin JM, Pathak VK. Mutations in the connection domain of HIV-1 reverse transcriptase increase 3′-azido-3′-deoxythymidine resistance. Proceedings of the National Academy of Sciences of the United States of America. 2007; 104:317–322. [PubMed: 17179211]
28. Nikolenko GN, Delviks-Frankenberry KA, Pathak VK. A novel molecular mechanism of dual resistance to nucleoside and nonnucleoside reverse transcriptase inhibitors. J Virol. 2010; 84:5238–5249. [PubMed: 20219933]
29. Nikolenko GN, Palmer S, Maldarelli F, Mellors JW, Coffin JM, Pathak VK. Mechanism for nucleoside analog-mediated abrogation of HIV-1 replication: balance between RNase H activity and nucleotide excision. Proceedings of the National Academy of Sciences of the United States of America. 2005; 102:2093–2098. [PubMed: 15684061]
30. Ohrui H, Kohgo S, Hayakawa H, Kodama E, Matsuoka M, Nakata T, Mitsuya H. 2′-Deoxy-4′-C-ethynyl-2-fluoroadenosine: a nucleoside reverse transcriptase inhibitor with highly potent activity